POLITECNICO
MILANO 1863

Modeling and control of power electronic converters for power systems applications

Student ID	Israa Mamoun Alsheikh Mohamed // 10618519
Supervisor	Prof. Giovanni Maria Foglia // Politecnico di Milano
Course	MSc electrical engineering
Faculty	Industrial and information engineering
Academic year	2021

This page is intentionally left blank

Assignment sheet for bachelor's thesis / master's thesis is inserted here

Skip this page when editing this template.

ACKNOWLEDGEMENT

I would like to acknowledge my gratitude and appreciation to Matej Krpan, Prof. Igor Kuzle from university of Zagreb and Prof. Giovanni Maria Foglia from university of Politecnico di Milano for being my supervisors during my journey. In the course of this process, you have given me a great amount of knowledge, experience and support.

I am also very grateful for the given opportunity of being a master student in both university of Zagreb and university of Politecnico di Milano. I got the chance to acquire an extraordinary learning experience, explored a new culture and made many good friends from several spots around the world.

At the end, I wish to express my deepest gratitude to my family, who's been a rock of stability throughout my life and for my friends who give me unconditional support. I am very grateful for your endless faith, love, sacrifices and support.

Table of Contents

List of figures

List of abbreviation

SC	Supercapacitor
ESS	Energy storage systems
CCM	Continuous conduction mode
DCM	Discontinuous conduction mode
PWM	pulse width modulation
SPWM	sinusoidal pulse width modulation
PLL	Phase locked loop
DQ0	Direct – quadrature – zero
VSI	Voltage source inverter
PCC	Point of common coupling

Modellazione e controllo di convertitori di elettronica di potenza per applicazioni di sistemi di alimentazione

Astratto

I convertitori per l'elettronica di potenza oggi svolgono un ruolo importante in un'ampia gamma di applicazioni, da piccole applicazioni a bassa potenza come telefoni, caricabatterie e alimentatori ad applicazioni di media scala come azionamenti per motori e fino a scale ad alta potenza e alta tensione come sistemi di generazione, autonomi e connessi alla rete. Ancora una volta, forniscono anche vantaggi sostanziali ai sistemi di alimentazione in termini di efficienza, affidabilità e risposta dinamica rapida. Questa tesi costituisce la modellazione e il controllo dei convertitori dell'elettronica di potenza nei sistemi di potenza in due fasi, la prima fase la parte di conversione DC DC per regolare la tensione DC. Il secondo stadio, è la conversione DC AC per controllare l'ampiezza e la frequenza della tensione AC sul lato della rete. Inoltre, viene implementato un controllo della potenza reale e reattiva attraverso lo schema di controllo corrente. La simulazione e la modellazione sono state implementate nella piattaforma Simulink.

Parole chiave:
Tesi di master; Elettronica di potenza; Convertitori CC-CC; Regolazione del voltaggio; inverter sorgente di tensione; controllo ad anello chiuso; schema di controllo attuale; e controllo della potenza reale e reattiva

Modeliranje i upravljanje istosmjernim i istosmjernim pretvaračima za primjenu u elektroenergetskim sustavima

Sažetak

Pretvarači energetske elektronike danas igraju glavnu ulogu u širokom spektru primjena, od male primjene male snage kao kod telefona, punjača i jedinica za napajanje, do primjene srednje razine kao u motornim pogonima i do skale visokog napona velike snage kao što je distribuirana proizvodni, samostalni i mrežni sustavi. Opet, oni također pružaju značajne prednosti elektroenergetskim sustavima u pogledu učinkovitosti, pouzdanosti i brzog dinamičkog odziva.

Ova teza predstavlja modeliranje i upravljanje pretvaračima energetske elektronike u elektroenergetskim sustavima u dva stupnja, prvi dio pretvorbe istosmjerne istosmjerne radi regulacije istosmjernog napona. Druga faza je DC izmjenična pretvorba za kontrolu amplitude i frekvencije izmjeničnog napona na strani mreže. Uz to, stvarna i reaktivna snaga upravljanja provodi se kroz trenutnu shemu upravljanja. Simulacija i modeliranje implementirano je u platformu Simulink.

Ključne riječi:

Magistarski rad, Energetska elektronika, pretvarači istosmjerne i istosmjerne struje, regulacija napona, pretvarač napona, upravljanje zatvorenim krugom, shema upravljanja strujom i regulacija stvarne i jalove snage

Modelling and control of power electronics converters for power system applications

Abstract

Power electronics converters nowadays play a major role in wide range of applications, from a small low power scale application as in phones, chargers and power supply units to medium scale applications as in motor drives and up to high power -high voltage scale such as distributed generation, standalone and grid connected systems. Again, they also provide substantial benefits to power systems in terms of efficiency, reliability, and fast dynamic response.

This thesis constitutes the modelling and controlling of the power electronics converters in power systems in two stages, first stage the DC DC conversion part in order to regulate the DC voltage. Second stage, is the DC AC conversion to control the amplitude and frequency of the AC voltage at the grid side. In addition, a real and reactive power control is implemented through current control scheme. The Simulation and modelling was implemented in Simulink platform.

Keywords:

Master's thesis; Power electronics; DC-DC Converters; Voltage regulation; Voltage source inverter; closed loop control; current control scheme; and real and reactive power control

1. Introduction

1.1 Background and Motivation

The growth of power electronics converters and the advantages they bring to the power systems in terms of efficiency, reliability and fast dynamic response is enormous. Moreover, there is wide range of applications - including large scale power systems such as distributed generation, standalone and grid connected systems- require the interface with power electronic devices in order to regulate and control the voltage and convert from DC to AC or vice versa. Hence, power electronic devices are becoming of bigger and bigger importance day after day.

In DC-DC converters, the average DC output voltage must be controlled to a desired level, though the input voltage and the output load may fluctuate. Switch-mode DC-DC converters utilize one or more switches to transform DC from one level to another. The average output voltage is controlled by controlling the switching duty cycle D [1].

The conversion of the regulated DC voltage to AC voltage connected to the grid is achieved through the DC AC inverter controlled by Pulse Width Modulation 'PWM' controller to give the desired output voltage and frequency at the grid side.

1.2 Thesis overview

In this thesis, modelling and simulation of DC-DC converter and DC-AC inverter has been conducted with an energy storage system (ESS) at the input side and a 3-phase grid at the output side. Fig. 1-1 illustrates the construction of the model.

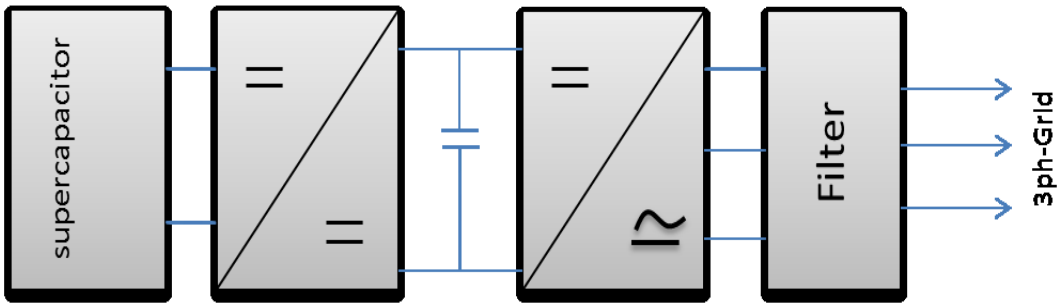

Figure 1-1: system description

1.3 Objectives

The thesis objectives can be summarized as follows:

1. To model and analyse the different types of DC-DC converters and with the interface of a supercapacitor ESS as DC input voltage.
2. To model, design and analyse the DC-AC inverter, and implementing SPWM technique to generate the desired amplitude and frequency for the AC output voltage.
3. To control the active and reactive power delivered to the grid.

1.4 Thesis Layout

The thesis is divided into four chapters including this introduction. A brief description of each chapter is as follows:

Chapter 2 includes the literature review and theoretical background which reflects on the design and different modelling scenarios of power electronic converters in general and DC-DC converters and DC-AC inverters specifically, and benefits when interfaced with the three-phase grid and renewable generation.

Chapter 3 provides detailed description of the modelling and simulation of each sub system – supercapacitor model, DC-DC converter, and DC-AC voltage source inverter (VSI)- along with the control for each subsystem. Then results are illustrated and discussed.

In Chapter 4 conclusions of the study are provided together with further steps that can be carried on.

2. Literature review

2.1 Supercapacitor model

Supercapacitor (SC) can be used in large scale application as part of hybrid energy storage system (ESS) for different reasons such as for micro grid application, for leveling out intermittent renewables in isolated systems or for frequency control as ancillary services.

For the study and the simulation of the given power systems the DC input is represented by means of energy storage system (ESS) and hence an accurate supercapacitor model has been considered to be quite applicable as it can be used for stabilization of intermittent output in case of renewable generation, and also when fast injection of high power is needed [4].

A simplified model of supercapacitor as shown in fig. 2-1 is constructed using two branches, first branch M1 represents the fast dynamics, added to it the second branch M2 which is slower recombination phenomena after a fast charge or discharge [4]

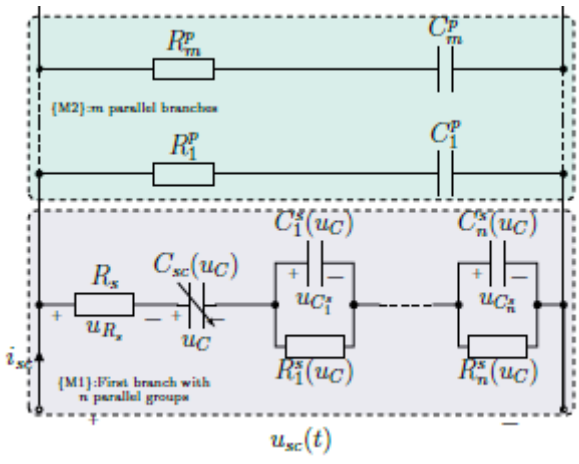

Figure 2-1: RC Circuit of supercapacitor cell
Source: [4]

The control and dynamic model for the SC is described in detail in [4], and the schematic diagram shown in fig. 2-2 where the input to the model of the supercapacitor is the current Isc (t) and output of the model is the SC terminal voltage Usc (t) [4].

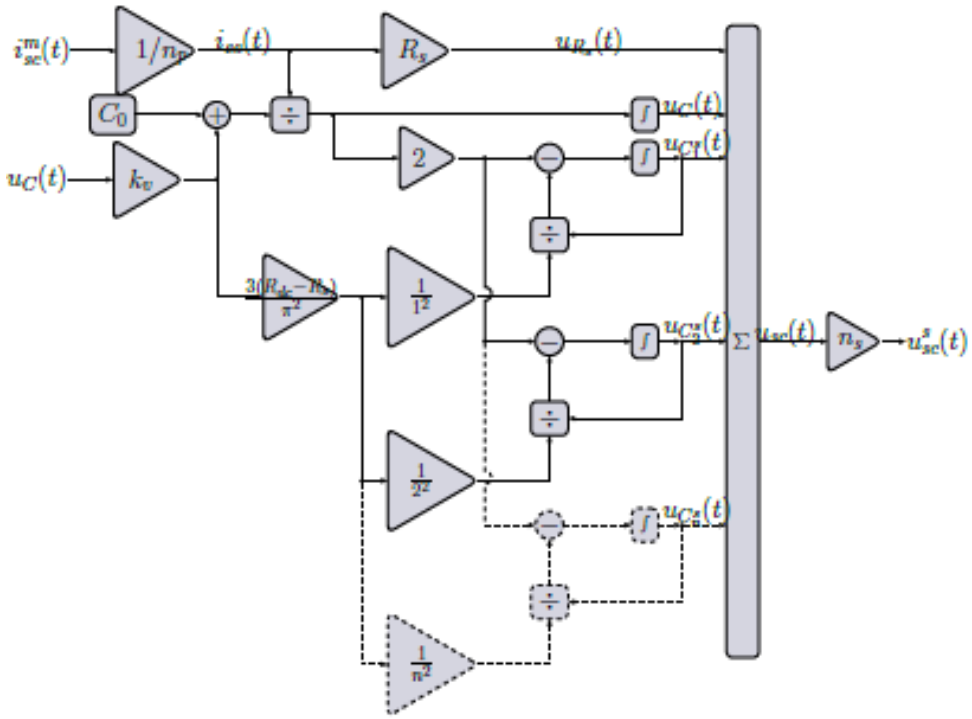

Figure 2-2: Diagram of the non-linear SC module model

Source: [4]

The output voltage of the SC module is very low voltage (< 3 V) and hence for large scale power systems, the model is to be scaled up by paralleling up to thousands SC module in case of > 1 MW supercapacitor banks.

2.2 DC-DC converter

The DC-DC converters are widely used in regulated switch-mode dc power supplies and in DC motor drive applications. Usually the input to these converters is an unregulated DC voltage that is obtained by rectifying the line voltage and therefore it will fluctuate due to changes in the line-voltage magnitude. Switch-mode DC-DC converters are used to convert the unregulated DC input into a controlled DC output at a desired voltage level [1].

There are several types of DC-DC converters, some are discussed below.

2.2.1 Step down - Buck converter:

The buck converter produces a lower average output voltage than the input DC voltage. Its main application is in regulated DC power supplies and DC motor speed control[1].

Conceptually, the basic circuit of Fig. 2-3 represents a buck converter for a purely resistive load. Assuming an ideal switch, a constant instantaneous input voltage V_D and a purely resistive load, the instantaneous output voltage curve is shown in Fig. 2-4 as a function of the switch position. The average output voltage can be calculated in terms of the switch duty ratio:

$$\boldsymbol{V_o = DV_D} \tag{2.1}$$

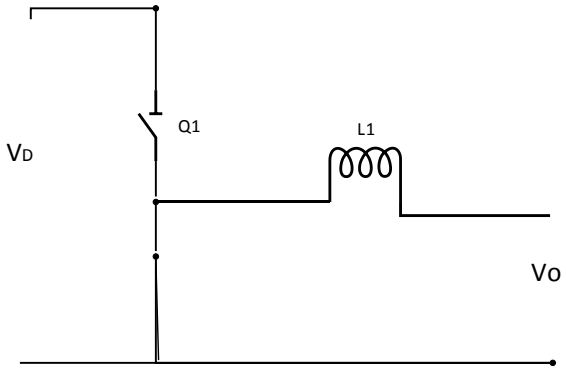

Figure 2-3: Basic circuit of buck converter

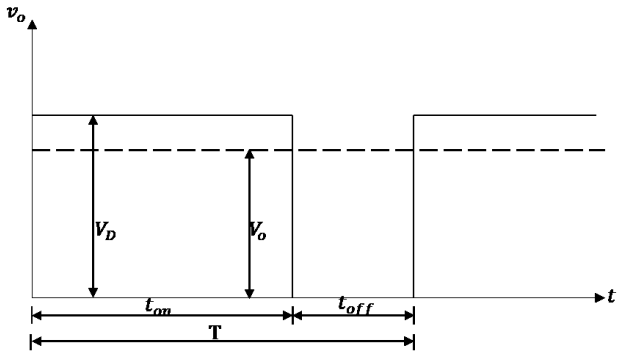

Figure 2-4: Output voltage waveform

2.2.2 Step-up - Boost converter:

Figure 2-5 shows a step-up converter. Its main application is in regulated dc power supplies and the regenerative braking of dc motors [1]. As the name implies, the output voltage is always greater than the input voltage. When the switch is on, the diode

is reversed biased, thus isolating the output stage. The input supplies energy to the inductor. When the switch is off, the output stage receives energy from the inductor as well as from the input. In the steady-state analysis presented here, the output filter capacitor is assumed to be very large to ensure a constant output voltage Vo (t) = *Vo.*

The average output voltage for the boost converter is given by:

$$V_o = \frac{1}{1-D} V_D \qquad (2.2)$$

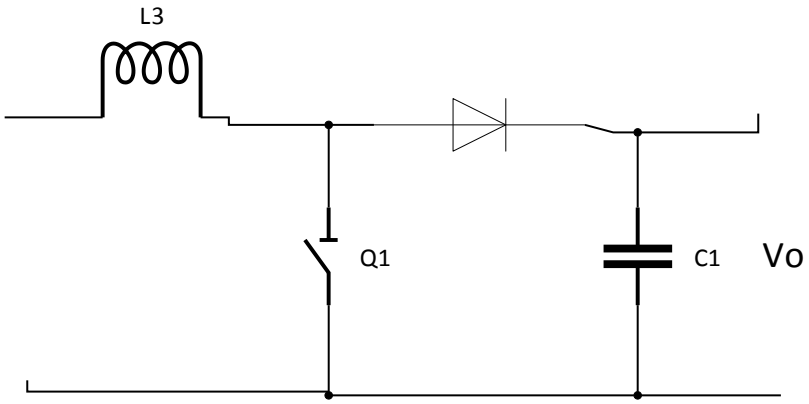

Figure 2-5: Basic Circuit of Boost converter

2.2.3 Buck-boost Converter (Inverting topology)

Another type of DC-DC converters is the buck-boost. The main application of a step-down/step-up or buck-boost converter is in regulated dc power supplies, where a negative-polarity output may be desired with respect to the common terminal of the input voltage, and the output voltage can be either higher or lower than the input voltage. A buck - boost converter can be obtained by cascading the connection of the two basic converters: the step-down converter and the step-up converter. In steady state, the output to input voltage conversion ratio is the product of the conversion ratios of the two converters in cascade [1].

The average output voltage for the boost converter is given by:

$$V_o = -\frac{D}{1-D} V_D \qquad (2.3)$$

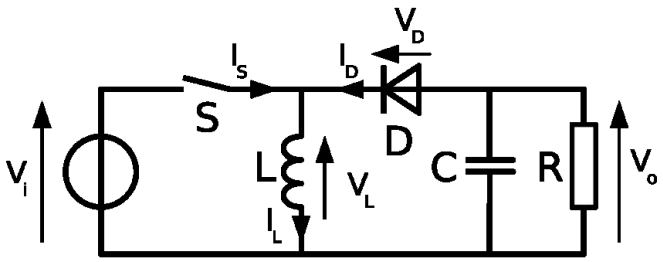

Figure 2-6: Inverting buck-boost converter circuit diagram

The circuit above fig. 2-6 shows a buck-boost converter with a negative output polarity and its magnitude can be greater or less than the input voltage according to the value of the duty cycle D.

2.2.4 Circuit averaging techniques (perturbation and linearization)

To achieve a time-invariant circuit layout, the main step in circuit averaging is to replace the converter switches with voltage and current sources [2]. The voltage and current generators' waveforms are defined to be identical to the original converter's switch waveforms. The converter waveforms can be averaged across one switching period to remove the switching harmonics once a time-invariant circuit network has been created. The averaged circuit model's nonlinear parts can then be disturbed and linearized, yielding the small-signal ac model [2].

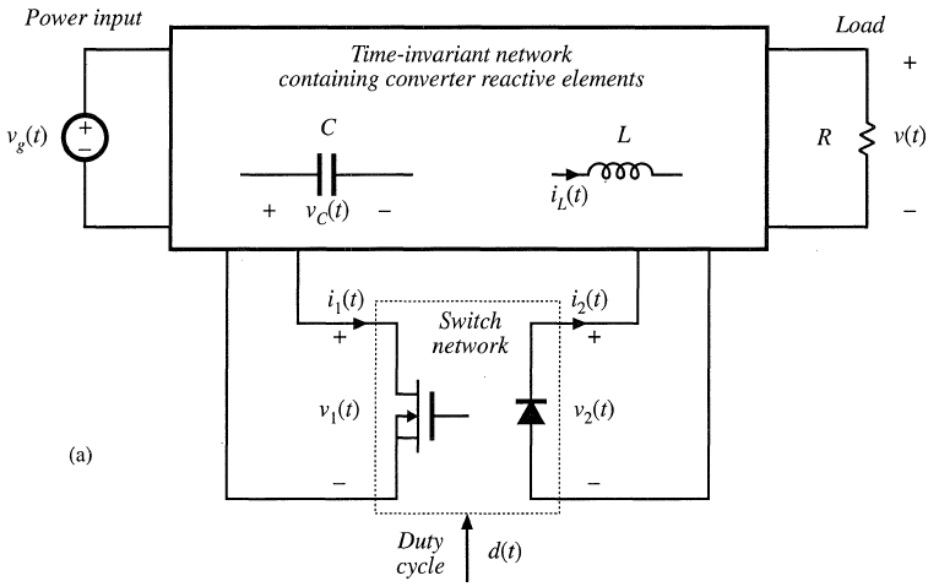

Figure 2-7: DC-DC converter with identified switch network

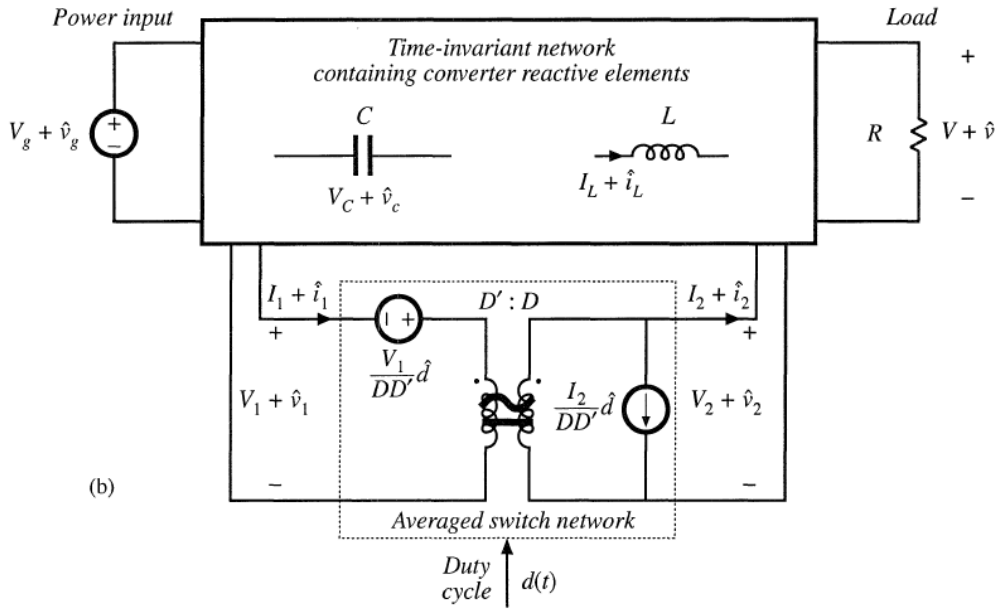

Figure 2-8: DC-DC converter with averaged switch network

To obtain the averaged model first the switch network is replaced by controlled voltage and current sources. Considering the averaged switch network shown in figure 2-8 above the input to the network is $v_1(t)$ = V_1+ $v(t)$ and the output is $v_2(t)$ = V_2+ $v(t)$ taking into account perturbation and linearization model.

$$\boldsymbol{v_1(t)} = \begin{cases} \boldsymbol{0} & \boldsymbol{0 < t < DT_s} \\ \boldsymbol{v_2(t)} & \boldsymbol{DT_s < t < T_s} \end{cases} \qquad (2.4)$$

Likewise in the output port the current through the inductor can be defined as:

$$\boldsymbol{i_2(t)} = \begin{cases} \boldsymbol{0} & \boldsymbol{0 < t < DT_s} \\ \boldsymbol{i_1(t)} & \boldsymbol{DT_s < t < T_s} \end{cases} \qquad (2.5)$$

Next, we remove the switching harmonics by averaging all signals over one switching period and assuming that the switching ripples of the inductor current and capacitor voltage are small, resulting in following equations:

$$\langle \boldsymbol{v_1(t)} \rangle = \boldsymbol{d'(t)} \langle \boldsymbol{v_2(t)} \rangle \qquad (2.6)$$

$$\langle \boldsymbol{i_2(t)} \rangle = \boldsymbol{d'(t)} \langle \boldsymbol{i_1(t)} \rangle \qquad (2.7)$$

Equations 2.6 & 2.7 above represents averaged model for the converter, this is a large signal nonlinear model.

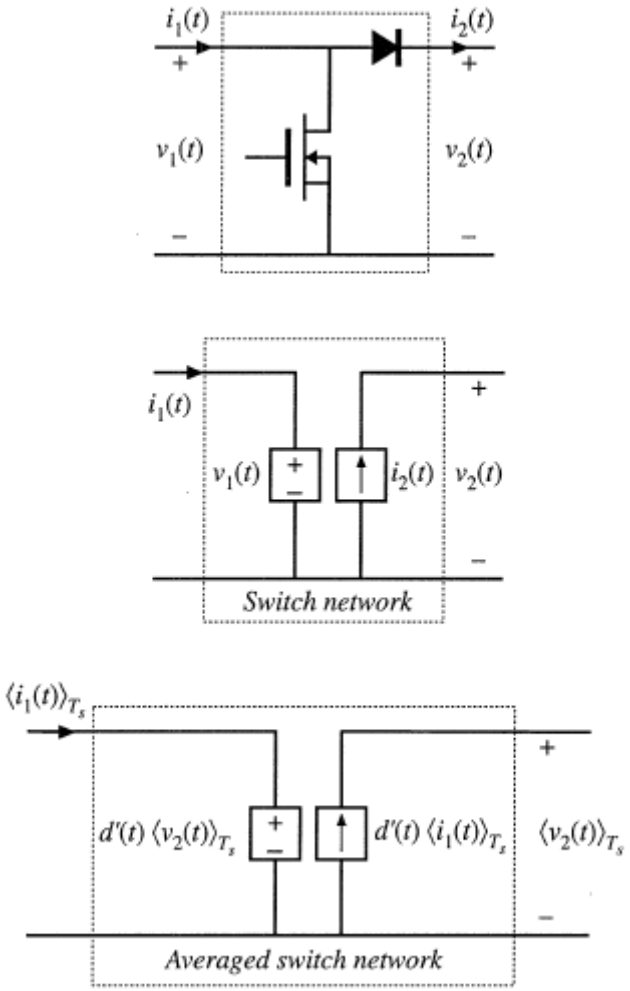

Figure 2-9: Derivation of the averaged switch model

2.2.5 Continuous conduction mode (CCM)

DC-DC converters can work in two modes, continuous conduction mode (CCM), where current is flowing continuously in the circuit and energy stored in the inductor does not reach zero. And discontinuous conduction mode (DCM) where energy stored in the inductor is completely discharged and current is zero before it starts to charge again in the next cycle. Considering a CCM, The values of the inductor and capacitor that determines the boundary between the CCM and DCM are:

$$\mathbf{L} = \frac{(\mathbf{1}-\mathbf{D})^{\mathbf{2}}\mathbf{R}}{\mathbf{2f}} \qquad (2.4)$$

$$C = \frac{D}{2 f R} \quad (2.5)$$

Where f is the frequency

2.2.6 Bidirectional DC-DC converter

In conventional converter the energy flows only in one direction, while bidirectional converter allows the flow of the energy in both directions. Also it can step up or step down the voltage based on either forward direction or backward direction. Bidirectional DC-DC converter is important in many application and specially when interfaced with ESS such as battery and supercapacitor to ensure the system reliability.

There are several types of the bidirectional converters, but the main concept realised in the switch. A bidirectional switch is illustrated in fig. 2-10, which is a MOSFET or IGBT switch that is connected anti-parallel with diode. This will allow the current to flow in both directions by means of controlled switching operation [2].

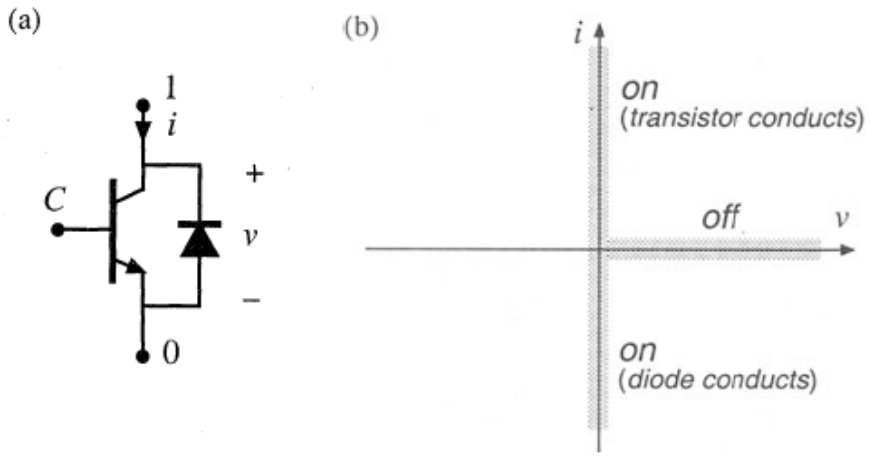

Figure 2-10: Two-quadrant SPST (a) switch construction (b) ideal characteristics source: [2]

2.2.7 Controlled Closed loop circuit

In a DC-DC converter application, it is desired to obtain a constant output voltage v(t) = V, in spite of disturbances in Vi(t) and i(t), and in spite of variations in the converter circuit element values.

To regulate the DC voltage, the converter is connected in closed loop circuit as shown in fig. 2-11 where a feedback from the output voltage is compared to a reference value of voltage and the error- difference- is sent to PI regulator to adjust the value of the duty cycle accordingly until we get the desired level of voltage [2].

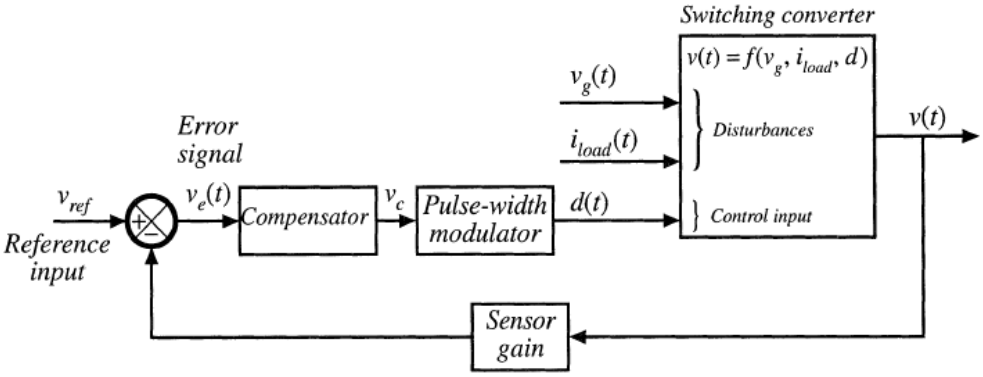

Figure 2-11: Closed loop control circuit.

Source: [2]

2.3 DC AC conversion

2.3.1 DC-AC Inverter

The inverter is used to convert the DC power from the DC-DC converter side to 3-phase AC power in the load side. For the three-phase inverter, 3 half bridge legs are connected.

Half bridge converter (single phase)

The half bridge converter is constructed from two switches, each paralleled with freewheeling diode, high side switch and low side switch. The two switches turn on/off alternatively to produce two level output voltage Vd/2 or –Vd/2. The circuit diagram for the half bridge converter is illustrated in fig. 2-12 below.

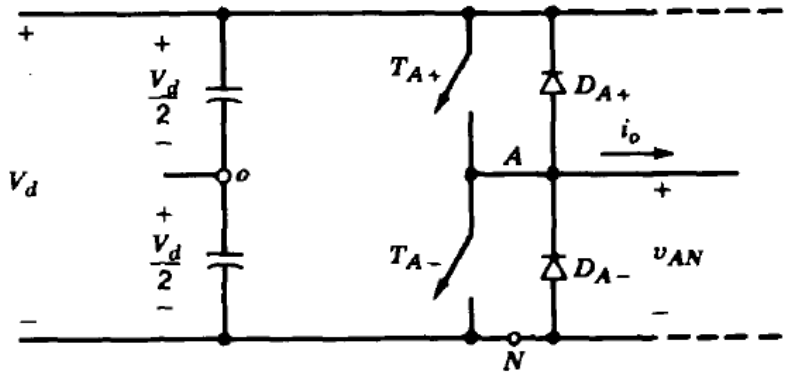

Figure 2-12: Inverter Half bridge configuration

Source: [1]

Three-phase Voltage sourced converter

The two level three phase VSI (shown in fig. 2-13) is constructed of three legs half bridge converters as one leg for each phase and the same principle of half bridge is applied with 120 degree phase shift between the legs. The control of the switching is realized by using SPWM that will be explained in the next section. This converter's power circuit arrangement is often called the six-pulse converter configuration.

The two-level VSC can provide a bidirectional power-flow path between the DC-side voltage source and the three phase AC system. The AC system can be passive, for example, an RLC load, or active, for example, a synchronous machine.

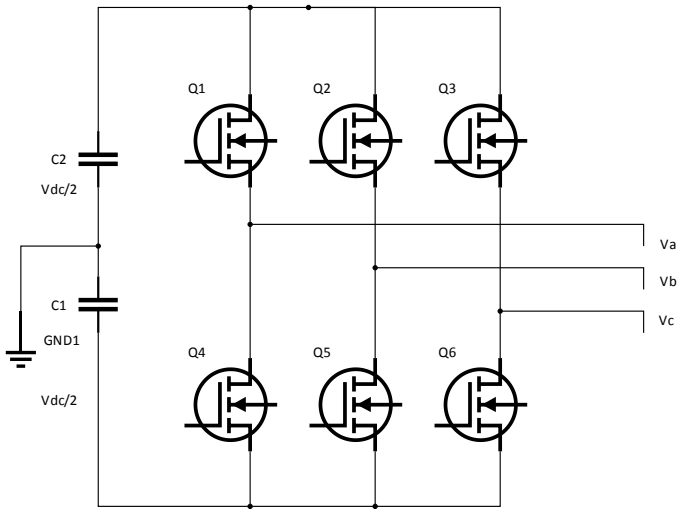

Figure 2-13: Three phase two levels voltage source inverter

2.3.2 Sinusoidal PWM

In inverter circuits, the PWM is a bit more complex than in DC-DC converters, since we would like the inverter output to be sinusoidal with controllable magnitude and frequency. In order to produce a sinusoidal output voltage waveform at a desired frequency, a sinusoidal control signal at the desired frequency is compared with a triangular waveform, as shown in Fig. 2-14 The frequency of the triangular waveform represents the inverter switching frequency and is generally kept constant along with its amplitude Vtri [1].

Before discussing the SPWM behaviour, it is necessary to define a few terms. The triangular waveform Vtri as shown in Fig. 2-15 establishes the frequency with which the inverter switches are switched *(fs* is also called the carrier frequency). The control signal Vcontrol is used to modulate the switch duty ratio and has a frequency f1, which is the desired fundamental frequency of the inverter output voltage (f1 is also called the modulating frequency), recognizing that the inverter output voltage will not be a perfect sine wave and will contain voltage components at harmonic frequencies of higher order. The amplitude modulation ratio *ma* and the modulation frequency index are defined as

$$ma = \frac{Vcontrol}{Vtri} \qquad \& \qquad mf = \frac{F_S}{F_1} \qquad (2.6)$$

Where (Vcontrol) is the peak amplitude of the control signal. The amplitude Vtri of the triangular signal is generally kept constant [1].

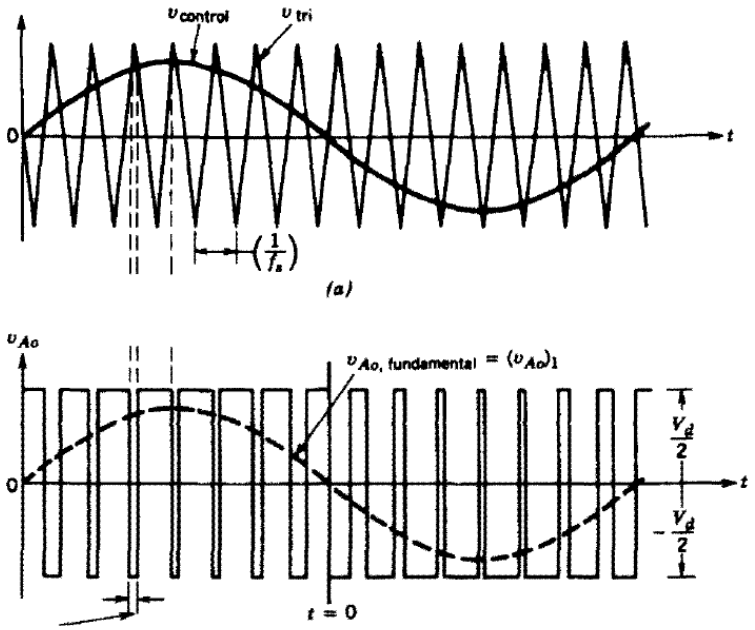

Figure 2-14: SPWM switching signal as a result of comparing the control signal with triangular signal [3]

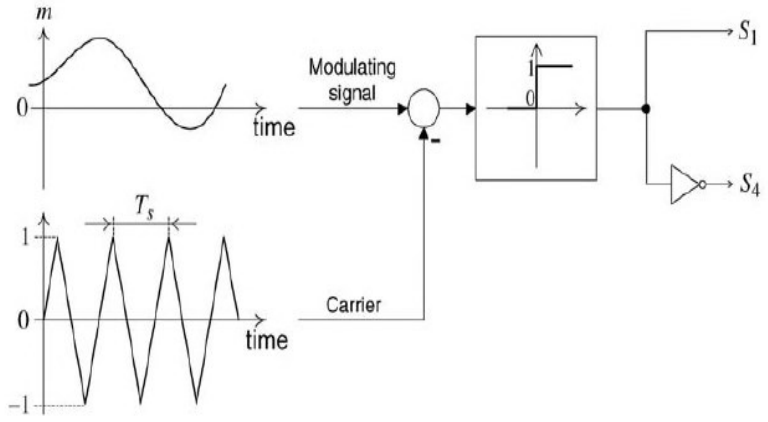

Figure 2-15: SPWM switching signal as a result of comparing the control signal with triangular signal [3]

2.3.3 Harmonics attenuation Filters:

The switching of the VSI results in harmonics which requires to be eliminated by use of filter. Either L or LC filters (fig. 2-16 & fig. 2-17) can be applied at the AC side for elimination of harmonics and to get sinusoidal voltage at the output. The filter is connected to the output of the inverter in order to attenuate high order harmonics and to

convert the square voltage waveform, into a sinusoidal waveform that meets the required standards. The filter is required to produce this output as well as incurring only minimal power loss. Therefore, the filter has to be constructed from reactive components, capacitors and inductors. The inductors must be constructed so that their windings have minimal resistance associated with them.

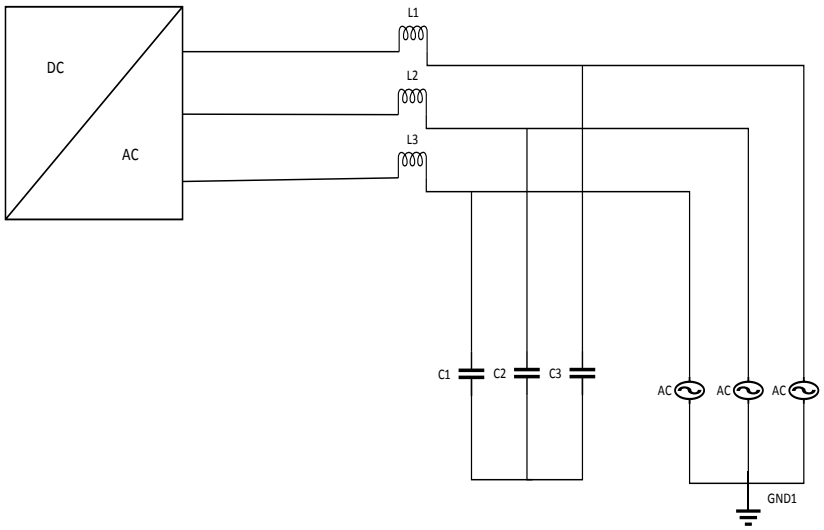

Figure 2-16: LC Filter schematic diagram

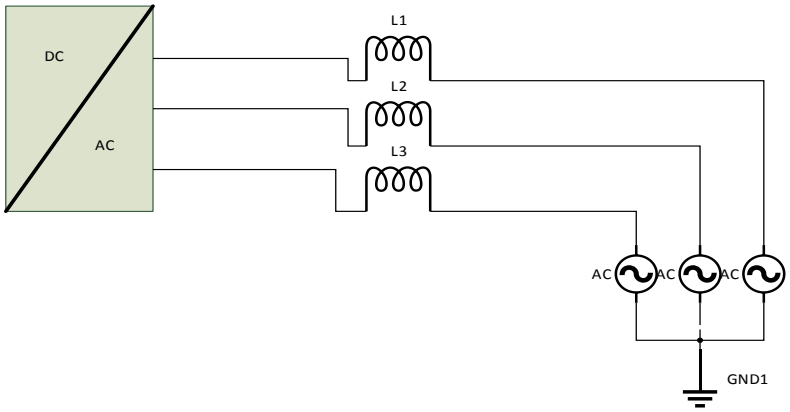

Figure 2-17: L filter schematic diagram

2.3.4 Closed loop control of the VSI

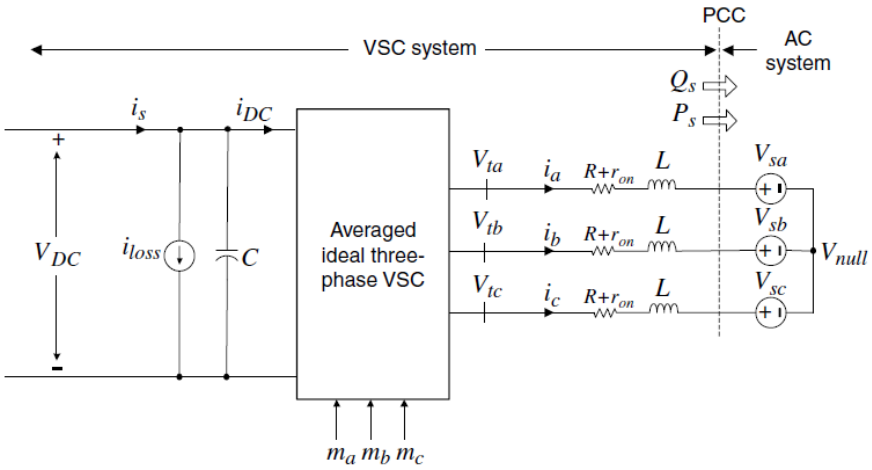

Figure 2-18: VSI system interfaced with the PCC

The control of the voltage source inverter regulates the voltage amplitude and frequency and hence controlling the reactive and active power delivered to the grid. The control should be implemented in D-Q reference frame instead of abc reference frame, this will reduce the number of plants to be controlled from 3 to 2, as well as completely decouple the control of the active and reactive power in balanced grid conditions. The transformation from abc reference frame to d-q reference frame is explained as following.

Alpha-beta transformation

The *αβ*-frame enables one to transform the problem of controlling a system of three half-bridge converters to an equivalent problem of controlling two equivalent subsystems. Moreover, the concept of instantaneous reactive power can be defined in the *αβ*-frame [3].

Consider the following balanced three phase quantity:

$$\begin{aligned} \boldsymbol{X_a(t)} &= \boldsymbol{X}\cos(\boldsymbol{\omega t}+\boldsymbol{\theta}) \\ \boldsymbol{X_b(t)} &= \boldsymbol{X}\cos(\boldsymbol{\omega t}+\boldsymbol{\theta}-\frac{\boldsymbol{2\pi}}{\boldsymbol{3}}) \\ \boldsymbol{X_c(t)} &= \boldsymbol{X}\cos(\boldsymbol{\omega t}+\boldsymbol{\theta}-\frac{\boldsymbol{4\pi}}{\boldsymbol{3}}) \end{aligned} \qquad (2.7)$$

A space phasor can now be defined as:

$$\vec{\boldsymbol{X}}\,(\boldsymbol{t}) = \hat{\boldsymbol{X}}\,\boldsymbol{e}^{-i\omega t} \qquad (2.8)$$

To retrieve the real values of the abc frame, the following formulas are used:

$$X_a(t) = Re\left\{\vec{X}\,(t)\,e^{-j0}\right\}$$
$$X_b(t) = Re\left\{\vec{X}\,(t)\,e^{-j\frac{2\pi}{3}}\right\}$$
$$X_c(t) = Re\left\{\vec{X}\,(t)\,e^{-j\frac{4\pi}{3}}\right\}$$

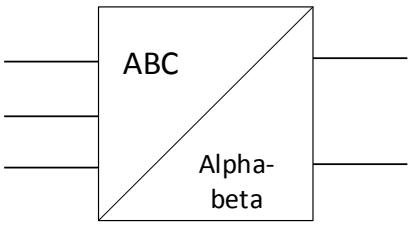

Figure 2-19: ABC reference frame to alpha-beta reference frame transformation

D-Q transformation

The transformation from the α-β reference frame to d-q reference frame is done by the following formula:

$$\boldsymbol{X_d} + \boldsymbol{jX_q} = (\boldsymbol{X_\alpha} + \boldsymbol{jX_\beta})\boldsymbol{e}^{-i\rho(t)} \qquad (2.9)$$

Where $\rho(t)$ represents the phase shift between the two frames. Which is obtained and control by the phase locked loop

The inverse transformation d-q to α-β reference frame is obtained by the following equation

$$\boldsymbol{X_\alpha} + \boldsymbol{jX_\beta} = (\boldsymbol{X_d} + \boldsymbol{jX_q})\boldsymbol{e}^{i\rho(t)} \qquad (2.10)$$

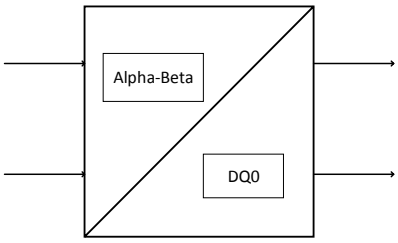

Figure 2-20: Alpha-beta reference frame to D-Q reference frame transformation

The D-Q frame control of a grid-imposed VSC system features all merits of the αβ-frame control, in addition to the advantage that the control variables are DC quantities in the steady state. This feature it remarkably facilitates the compensator design, especially in variable-frequency scenarios [3].

2.3.5 Real and reactive power controller

Real and reactive power exchanged between the VSI and the three phase grid, need to be controlled instantaneously. Mainly there are two methods of controlling the real and reactive power in the VSI system. The first method is the voltage-mode control and has been dominantly utilized in high-voltage/-power applications such as in FACTS [3]. The schematic diagram for the voltage mode control is illustrated in fig. 2-21. As can be seen from the schematic diagram the voltage-mode control is simple and has a low number of control loops. However, the main drawback of the voltage-mode control is the absence of control loop closed on the VSC line current. This will lead to lack of protection against over-currents, and the current may undergo large excursions if the power commands are rapidly changed or faults take place in the AC system [3].

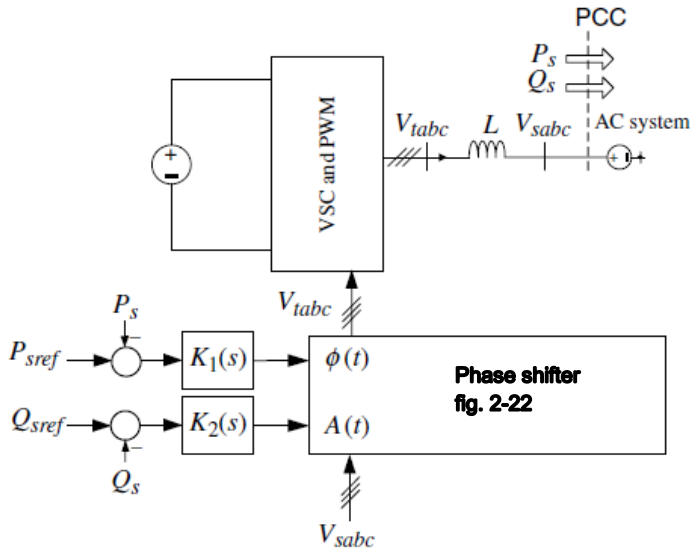

Figure 2-21: Schematic diagram for voltage mode control for real reactive power controller

Source: [3]

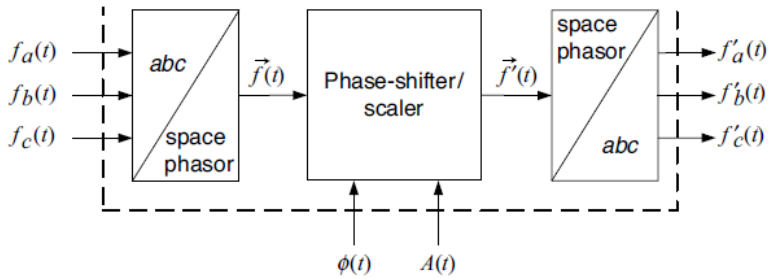

Figure 2-22: Phase shifter source [3]

The second method of controlling the real and reactive power is current mode control as illustrated in fig. 2-23. This approach will then be considered here as the mean of the controlling the real and reactive power. Due to the current regulation scheme, the VSC is protected against overcurrent conditions. Moreover, current-mode control includes robustness against variations in parameters of the VSC system and the AC system, superior dynamic performance, and higher control precision [3].

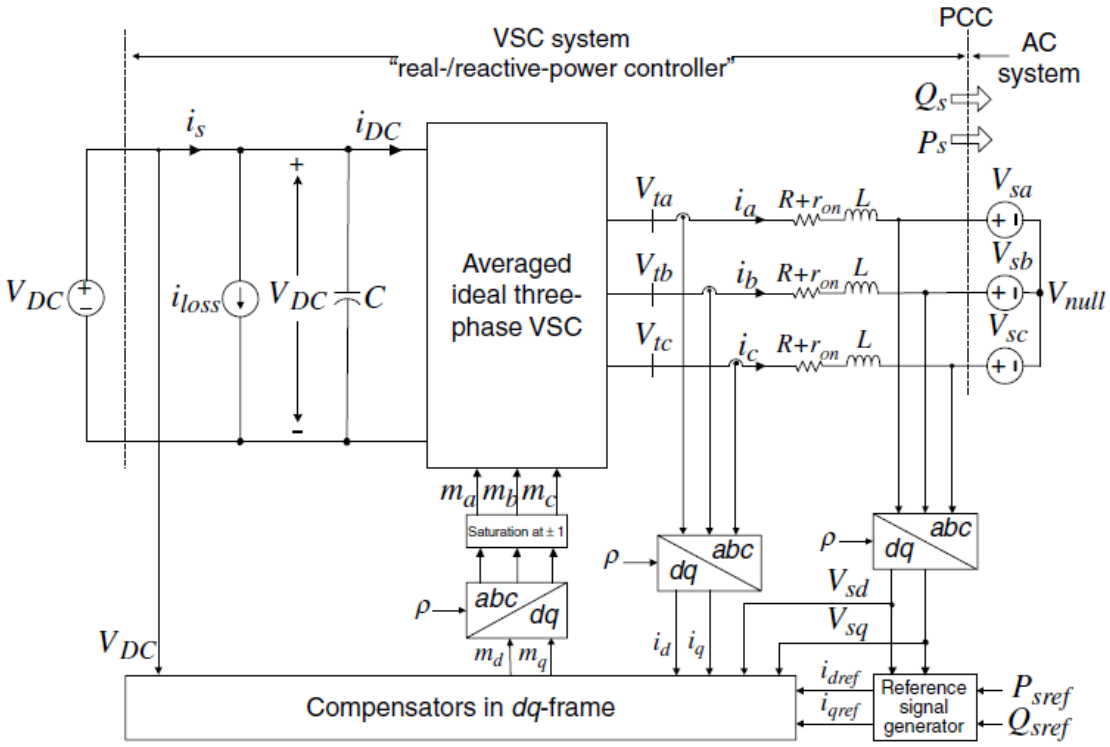

Figure 2-23: Schematic diagram of real and reactive power control system

Source: [3]

The real and reactive powers are controlled by the phase angle and the amplitude of the VSC line current with respect to the point of common coupling (PCC) voltage. Thus, due to the current regulation scheme, the VSC is protected against overcurrent conditions. Other advantages of the current-mode control include robustness against variations in parameters of the VSC system and the AC system, superior dynamic performance, and higher control precision [3].

Assume the grid voltage in abc frame as following:

$$V_a(t) = \hat{V}\cos(\omega t + \theta)$$
$$V_b(t) = \hat{V}\cos(\omega t + \theta - \tfrac{2\pi}{3}) \qquad (2.11)$$
$$V_c(t) = \hat{V}\cos(\omega t + \theta - \tfrac{4\pi}{3})$$

Where $\hat{V}$ is the peak value of the line-to-neutral voltage, ω is the AC system (source) frequency, and θ is the source initial phase angle. Hence, the space-phasor equivalent of *Vs−abc* is:

$$\vec{V}\,(t) = \hat{V}\, e^{-i(\omega t+\theta)} \tag{2.12}$$

The dynamics of the AC side of the inverter can be described in space phasor by the following equation:

$$\mathbf{V_t} - \mathbf{V_s} = \mathbf{L}\,\frac{\mathbf{di}}{\mathbf{dt}} + \mathbf{Ri} \tag{2.13}$$

Substituting V_s as in (2.12):

$$L\,\frac{di}{dt} = -Ri + V_t - \hat{V}\, e^{-i(\omega t+\theta)} \tag{2.14}$$

Expressing (2.14) in d-q frame:

$$L\frac{d(i_{dq}\, e^{i\rho})}{dt} = -R\left(i_{dq}\, e^{i\rho}\right) + V_{tdq} e^{i\rho} - \hat{V}\, e^{-i(\omega t+\theta)} \tag{2.15}$$

(2.15) can be rewritten as the following:

$$L\frac{d(i_{dq})}{dt} = -j\left(L\frac{d\rho}{dt}\right) i_{dq} - R\left(i_{dq}\right) + V_{tdq} - \hat{V}\, e^{-i(\omega t+\theta-\rho)} \tag{2.16}$$

Decomposing (2.16) into real and imaginary components:

$$L\frac{d(i_d)}{dt} = -L\frac{d\rho}{dt} i_q - R(i_d) + V_{td} - \hat{V}\,\cos(\,\omega t + \theta - \rho) \tag{2.17}$$

$$L\frac{d(i_q)}{dt} = -L\frac{d\rho}{dt} i_d - R\left(i_q\right) + V_{tq} - \hat{V}\,\sin(\omega t + \theta - \rho) \tag{2.18}$$

At steady state $\frac{d\rho}{dt} = \omega(t)$ and thus equations (2.17) & (2.18) can be written as:

$$L\frac{d(i_d)}{dt} = -L\omega(t) i_q - R(i_d) + V_{td} - \hat{V}\,\cos(\,\omega t + \theta - \rho) \tag{2.19}$$

$$L\frac{d(i_q)}{dt} = -L\omega(t) i_d - R\left(i_q\right) + V_{tq} - \hat{V}\,\sin(\omega t + \theta - \rho) \tag{2.20}$$

In (2.19)–(2.20), *id*, *iq*, and *ρ* are the state variables, V_{td} , V_{tq} and *ω* are the control inputs. The system described by (2.19)–(2.20) is nonlinear due to the presence of the terms ωi_d, ωi_q, $\cos(\ \omega t + \theta - \rho)$ and $\sin(\omega t + \theta - \rho)$

In (2.19) & (2.20)

$$V_{sd} = \hat{V}\ \cos(\ \omega t + \theta - \rho) \qquad (2.21)$$

$$V_{sq} = \hat{V}\ \sin(\ \omega t + \theta - \rho) \qquad (2.22)$$

Hence,

$$L\frac{d(i_d)}{dt} = \ -L\omega(t)i_q - R(i_d) + \ V_{td} - V_{sd} \qquad (2.23)$$

$$L\frac{d(i_q)}{dt} = \ -L\omega(t)i_d - R(i_q) + \ V_{tq} - V_{sq} \qquad (2.24)$$

Which describe a second-order linear system that is excited by the constant input Vs. Thus, if V_{td} and V_{tq} are DC variables, id and iq are also DC variables in the steady state. The mechanism to ensure ρ(t) = ω0t + θ0 is referred to as the PLL [3]. The following section presents the structure, model, and stabilization of the PLL.

2.3.6 Phase locked loop (PLL) control:

In PLL the goal is to keep $\rho(t) = \ \omega t + \theta$ and correspondingly, $V_{sq} = 0$.

Therefore, we devise a mechanism to regulate *Vsq* at zero. This can be achieved based on the following feedback law:

$$\omega(t) = H(\rho)V_{sq} \qquad (2.25)$$

Where *H*(*ρ*) is a linear transfer function (compensator) and *p* = *d*(·)*/dt* is a differentiation operator. Substituting for $V_{sq}$from (2.22) in (2.25), and substituting *ω* by $\frac{d\rho}{dt}$:

$$\frac{d\rho}{dt} = H(\rho)\hat{V}\ \sin(\ \omega t + \theta - \rho) \qquad (2.26)$$

Equation (2.26) describes a non-linear dynamic system which is PLL. The function of the PLL is to regulate ρ at ω0t + θ0. However, in view of its nonlinear characteristic, the PLL can exhibit unsatisfactory behaviour and limit cycle under certain conditions. Hence, to avoid this from happening, the control law can be adjusted by adding the limit constrains:

$$\omega(t) = H(\rho)\ Vsq(t),\ \omega(0) = \omega 0 \text{ and } \omega\ \min \le \omega \le \omega\ \max \qquad (2.27)$$

where ω(t) has the initial value ω(0) = ω0 and is limited to the lower and upper limits of, respectively, ω min and ω max. ω min and ω max are selected to be close to ω0 and thus to define a narrow range of variations for ω(t) [3].

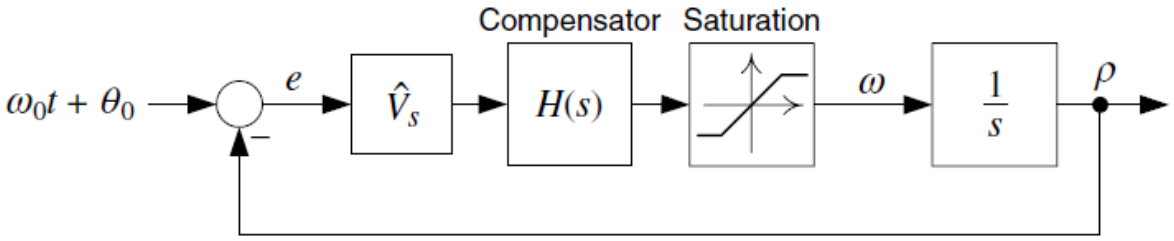

Figure 2-24: Control block diagram of PLL [3]

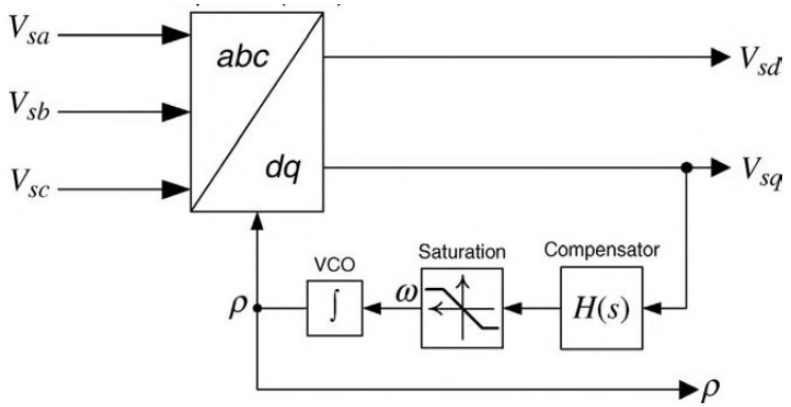

Figure 2-25: PLL controller schematic diagram [3]

Figure 2-25 shows that the PLL transforms *Vsabc* to *Vsdq* and adjusts the rotational speed of the *dq*-frame, that is, *ω*, such that *Vsq* is forced to zero in the steady state. The end result is that *ρ* = *ω*0*t* + *θ*0 and *Vsd* = *Vs*.

2.3.7 Current control scheme for real and reactive power

The real and the reactive power at the load side PCC point of common coupling are given by the following equations:

$$P(t) = \frac{3}{2}(V_{sd}\, i_d + V_{sq}\, i_q) \qquad (2.28)$$

$$Q(t) = \frac{3}{2}(-V_{sd}\, i_q + V_{sq}\, i_d) \qquad (2.29)$$

Where V_{sd} & V_{sq} , are the DC components of the AC voltage at the grid side (PCC). For a steady state PLL, where V_{sq} is equal to zero, the real and reactive power will be given by:

$$P(t) = \frac{3}{2}(V_{sd}\, i_d) \qquad (2.30)$$

$$Q(t) = \frac{3}{2}(-V_{sd}\, i_q) \qquad (2.31)$$

From the above equations it can be seen that real and reactive power can be controlled by controlled the DQ component of the current at the output of the inverter. And in order to get the reference currents, reference real and reactive power can be used as following

$$i_d = \frac{2}{3V_{sd}}\, Pref \qquad (2.32)$$

$$i_q = -\frac{2}{3V_{sd}}\, Qref \qquad (2.33)$$

Then, if the control system can provide fast reference tracking, that is, id ≈ idref and iq ≈ iqref , then P ≈ Pref and Q ≈ Qref , that is, P(t) and Q(t), can be independently controlled by their respective reference commands. Since Vsd is a DC variable (in the steady state), idref and iqref are also DC variables if Pref and Qref are constant signals. Thus, as expected, the control system in D-Q frame deals with DC variables, unlike the control system in αβ-frame that deals with sinusoidal signals [3].

From the VSI model it can be written the DQ components of the AC voltage as following:

$$V_{td} = \frac{V_{dc}}{2}\ m_d(t) \qquad (2.34)$$

$$V_{tq} = \frac{V_{dc}}{2}\ m_q(t) \qquad (2.35)$$

To deduce $m_d(t)$ and $m_q(t)$ we can substitute the V_{td} and V_{tq} as shown in the following equations:

$$m_d(t) = \frac{2}{V_{dc}}(u_d - l\omega i_q + V_{sd}) \qquad (2.36)$$

$$m_q(t) = \frac{2}{V_{dc}}(u_q + l\omega i_d + V_{sq}) \qquad (2.37)$$

Where u_d and u_q are adjusted by the PI regulators to get the desired values for i_d and i_q. Fig. 2-26 shows the control block diagram for the current controlled VSI system.

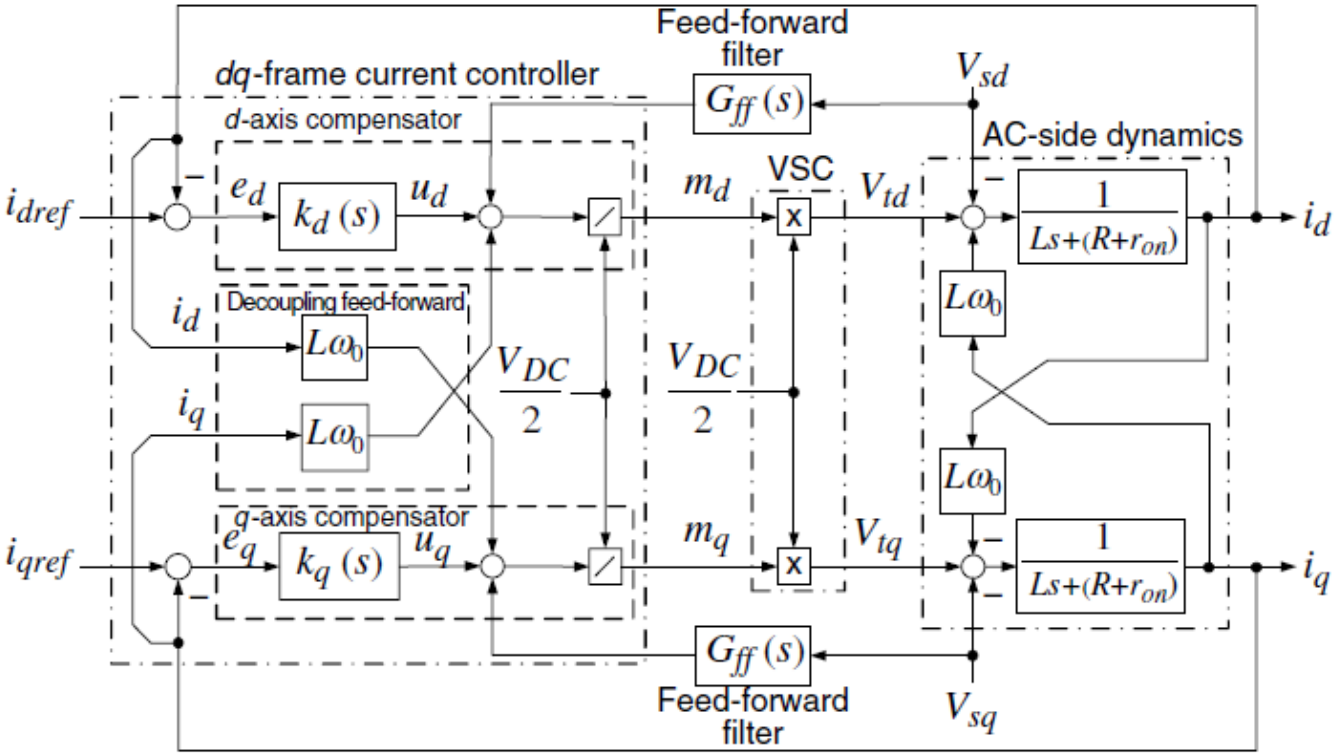

Figure 2-26: VSI Current control block diagram

Source: [3]

A simplified current control block diagram can be shown in fig. 2-27

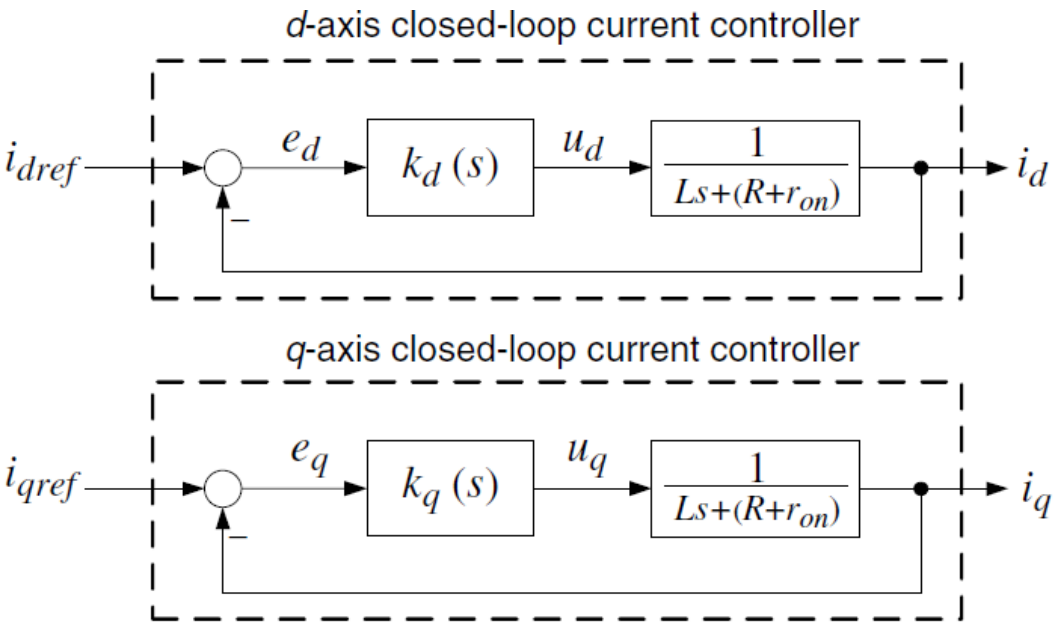

Figure 2-27: Simplified VSI current control block diagram

Source: [3]

3. Modelling, simulation and results

3.1 Supercapacitor:

A supercapacitor model representing an ESS (energy storage system) with an output voltage of 2.7 V is connected to our DC-DC converter. Fig. 3-1 shows the block of the supercapacitor with its interface with the DC-DC converter which is controlled by PWM controller generating signal S1 and signal S2. The input current to the supercapacitor is feedback from the current measurement at the output side of the supercapacitor. For a desired input voltage of 1000 V at the converter input side 370 supercapacitors were connected in series.

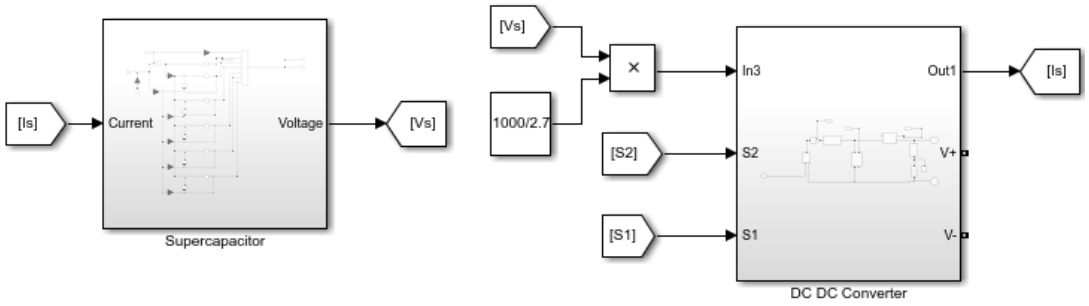

Figure 3-1: supercapacitor model interfaced with the DC-DC converter

The detailed model of the supercapacitor is illustrated in figure. 2-2.

3.2 DC-DC converter

Different types and scenarios for DC-DC converters have been analysed and modelled.

3.2.1 Inverting Buck boost converter

Buck boost model has been considered to regulate the DC input voltage at the required level and hence to be able to step up or down the voltage as required. The model which has been designed is the typical inverting buck boost which gives a negative output. The design of the converter is based on the switching frequency which

is chosen to be 100 KHz. The input voltage to the converter is the output of the supercapacitor and considered to be in the range 1000 - 1500 V min-max voltage. Considering a continuous conduction mode CCM, and by considering a limit for the current ripple to be less than half the average current the inductance is calculated as shown in (3,2). Assuming also a limit for the voltage ripple the capacitance are calculated as shown in (3.5) [1].

$$D = \frac{V_o - V_i}{V_o} \qquad (3.1)$$

$$L \geq D \frac{V_{in\_min}}{\Delta i * F_S} \qquad (3.2)$$

$$\Delta i = 0.4\, I = 0.1 * \frac{P}{V_{in\_min}} \qquad (3.3)$$

$$\therefore \mathrm{L} \geq \mathrm{D} \frac{\mathrm{V_{in\_min}}^2}{0.1\mathrm{P} * \mathrm{F_S}} \qquad (3.4)$$

$$\therefore \mathrm{C} \geq \frac{\mathrm{D} * \mathrm{V_o}}{0.01 * \mathrm{R} * \mathrm{F_S}} \qquad (3.5)$$

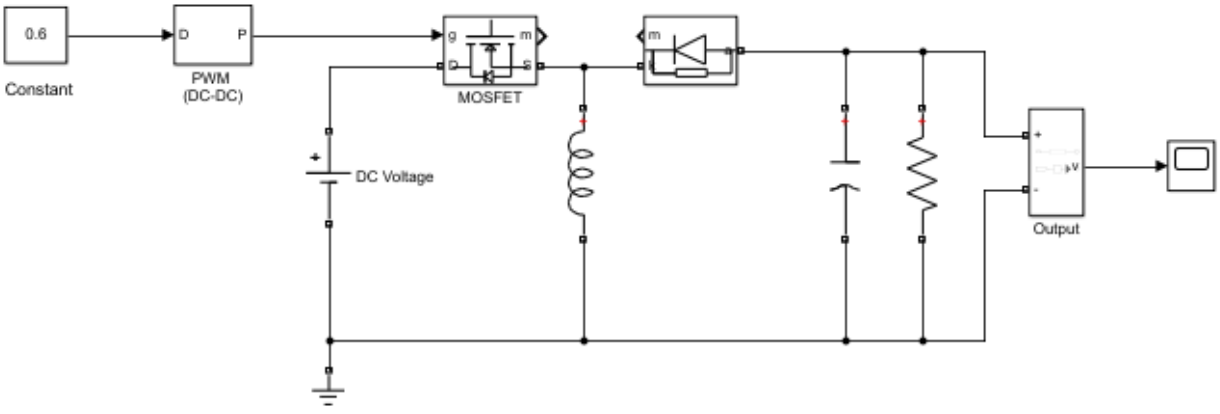

Figure 3-2: Inverting Buck Boost Model

The regulated DC voltage at the output is found to be around - 1500 V with switching ripple +/- 50 volt as shown in fig-3-3 below.

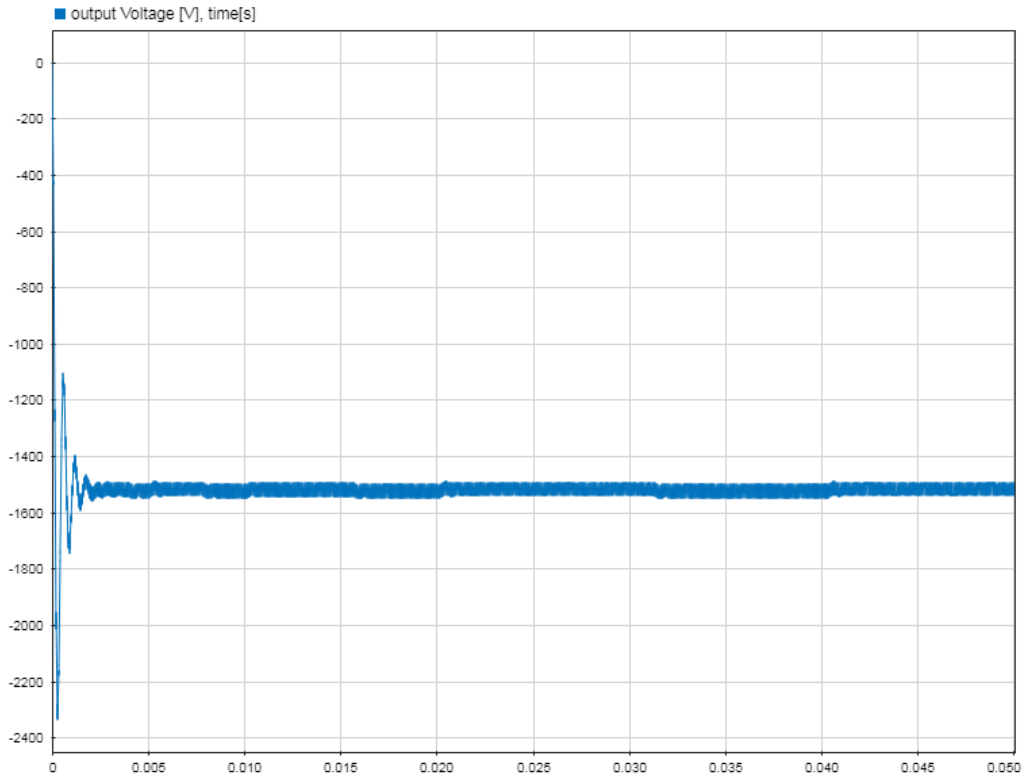

Figure 3-3: Inverting buck boost Output Voltage

By interfacing the buck boost converter above to the supercapacitor as the input DC voltage as shown in figure 3-4, it can be seen that the resulted DC output voltage is regulated around 1500 V as shown in figure 3-5.

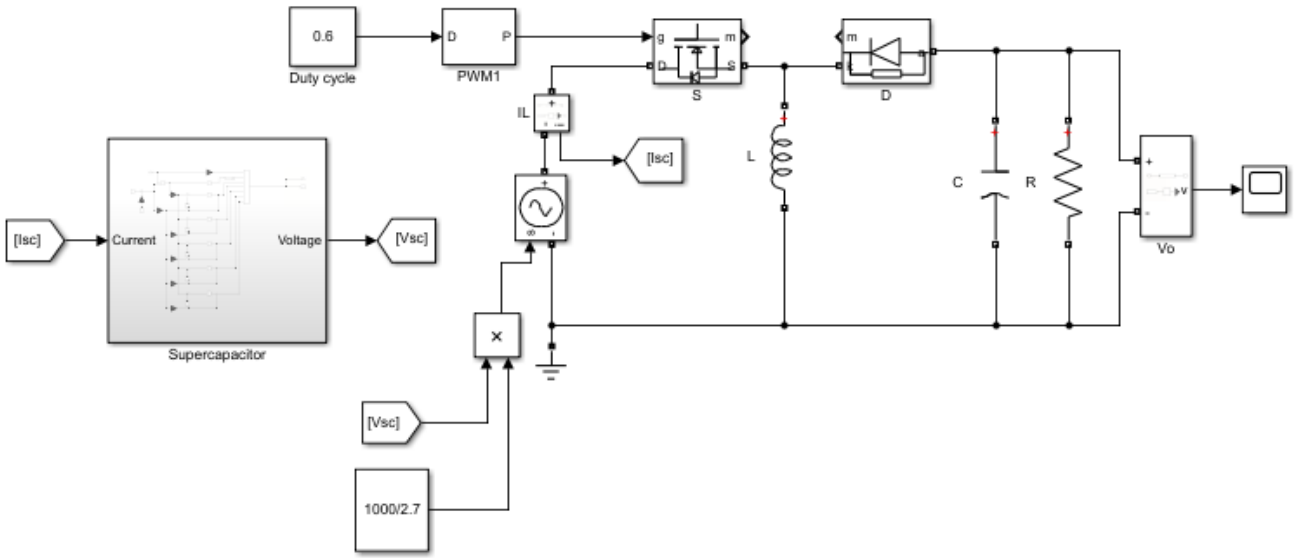

Figure 3-4: Buck boost converter with SC interface

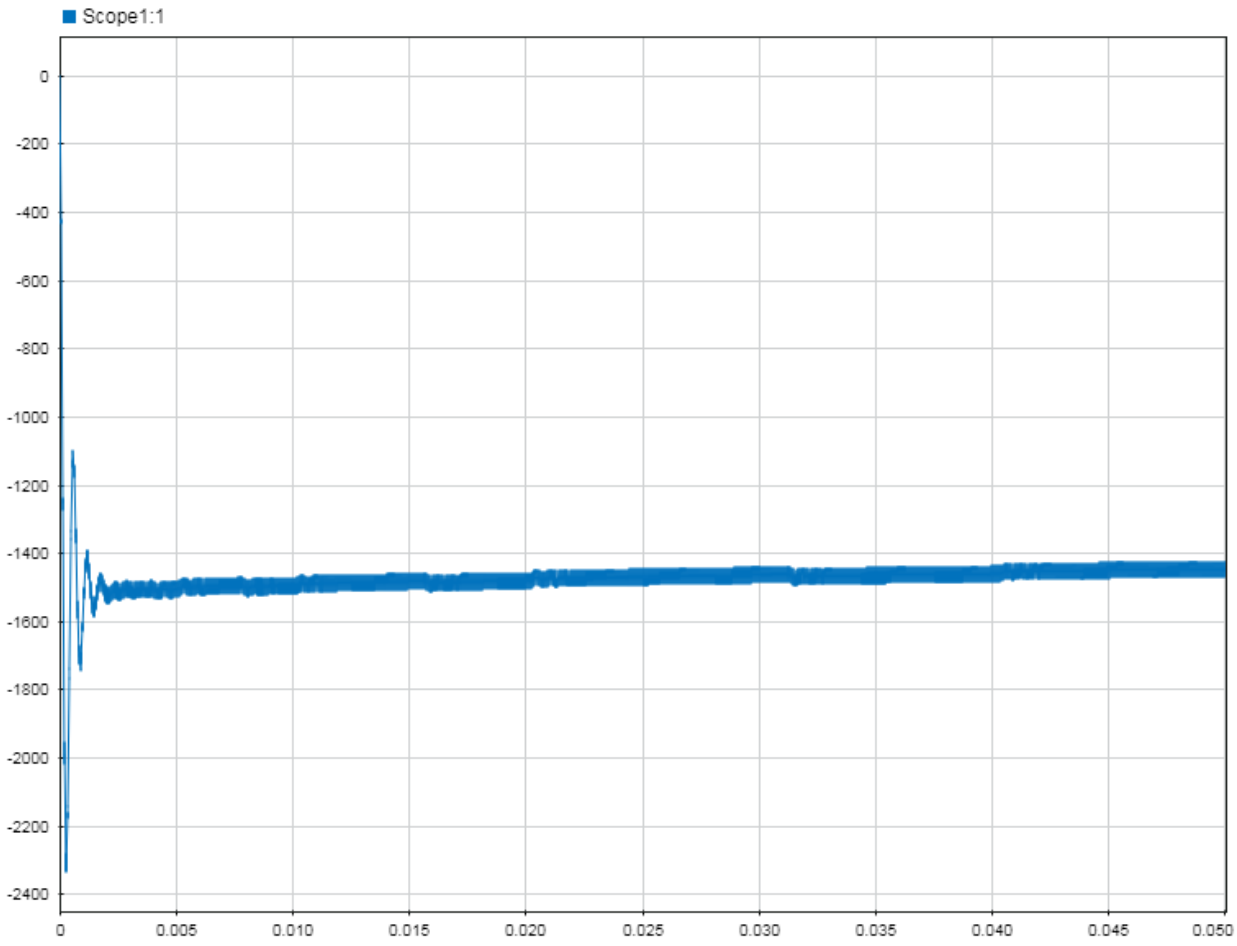

Figure 3-5: Output DC voltage

3.2.2 Non-switched model

In order to have an averaged model which removes switching harmonics by averaging all signals over switching period, the switched network (MOSFET + diode) is replaced by voltage controlled source and current controlled source. Figure 3-6 below shows the equivalent circuit after applying the same concept illustrated in chapter 2, sections 2.2.4.

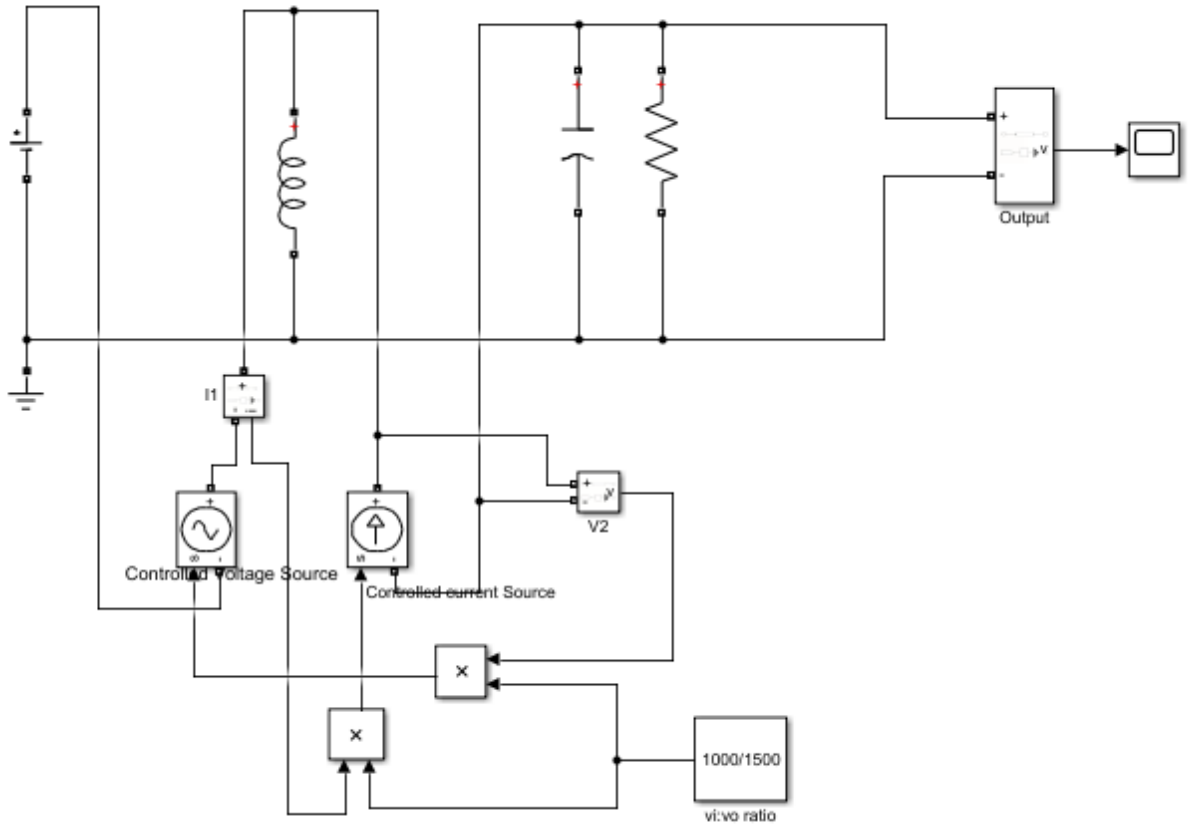

Figure 3-6: DC-DC Converter averaged switch model

Considering a ratio of conversion for the switching network 1:D = V_i : V_o = 1000/1500, the resulted voltage at the output as illustrated in figure 3-7 below shows regulated DC voltage with less switch ripples compared to regular buck-boost model.

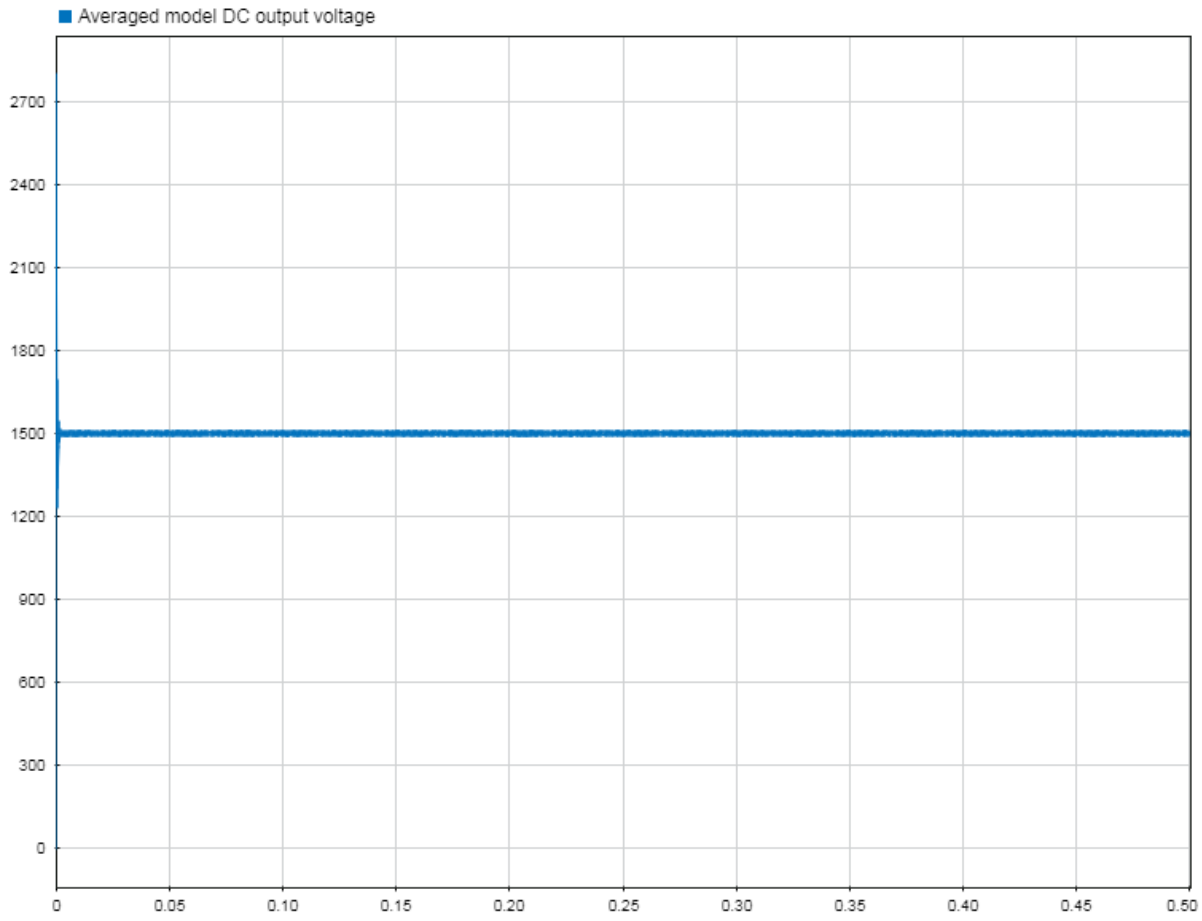

Figure 3-7: Output voltage of the averaged non switched model

Next the unregulated DC input is introduced as interface from the supercapacitor model and multiplied by 1000/2.7 factor to get the 1000 V input as shown in figure 3-8. Below:

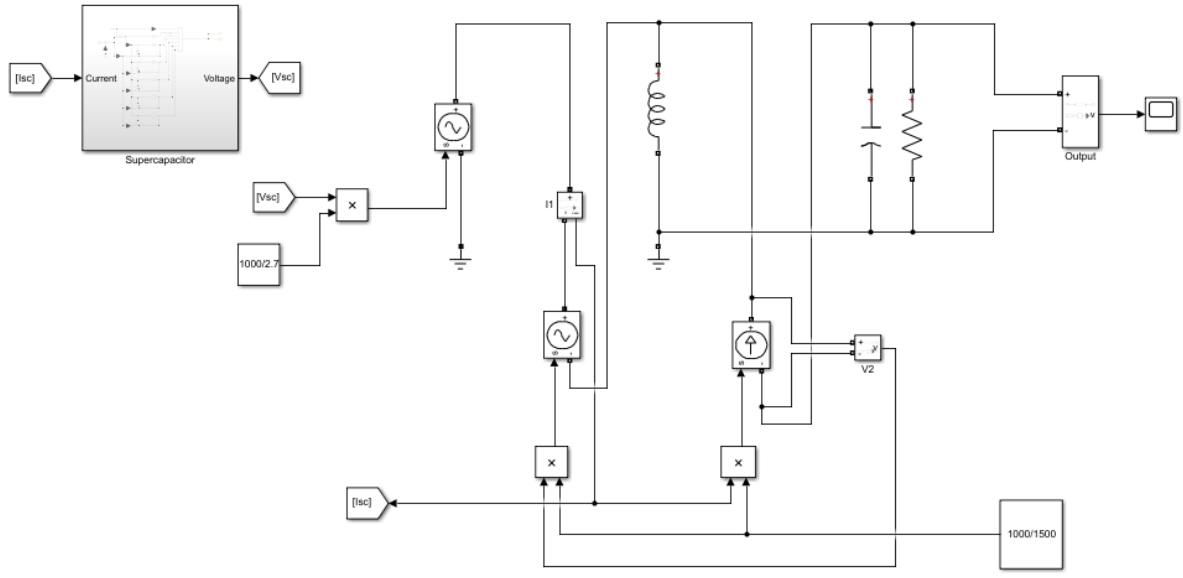

Figure 3-8: Non switched model with SC interfaced at the input side

As a result, the DC output voltage (Fig. 3-9) shows less switching ripple compared to switched model.

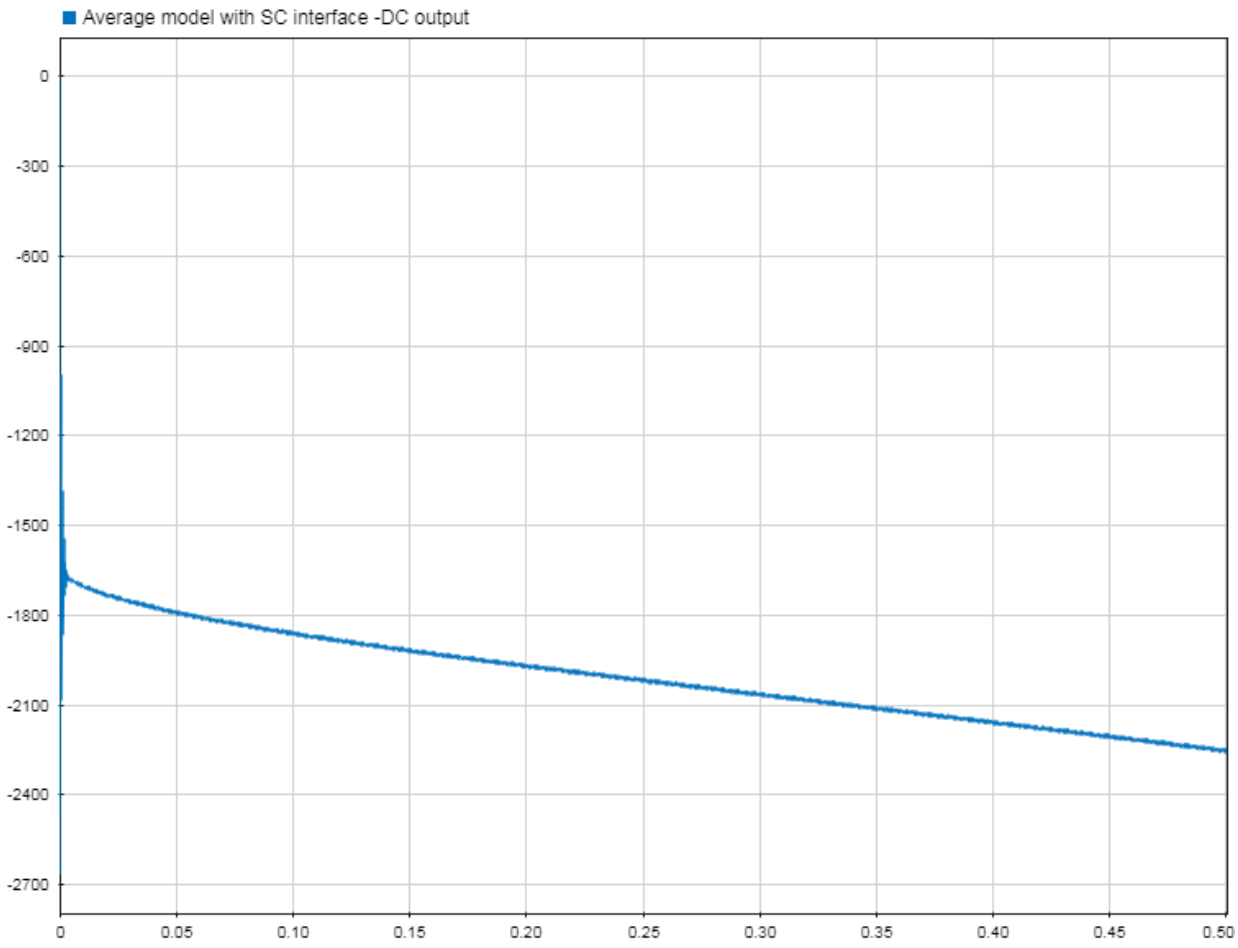

Figure 3-9: Output voltage of averaged model with SC

3.2.3 Bidirectional boost converter

A boost converter has been considered for its simplicity and as the most diffused type of converters. The step up converter has been modelled and designed to increase the DC input voltage from 500-1000 V to 1500 V. The bidirectional boost converter is constructed as shown in fig. 3-10 below, with two switches to allow the bi-directionality of the converter, input 1 is the voltage from the supercapacitor. The design of the converter is based on the switching frequency which is chosen to be 100 KHz. The input voltage to the converter is the output of the supercapacitor and considered to be in the range 1000 - 1500 V min-max voltage. Considering a continuous conduction mode CCM, and by considering a limit for the current ripple to be less than half the average current the inductance is calculated as shown in (3,2). Assuming also and limit for the voltage ripple the capacitance are calculated as shown in (3.5) [1]:

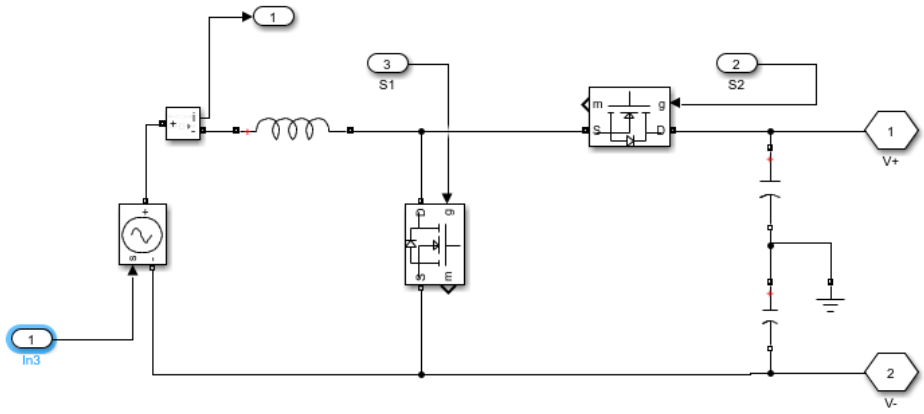

Figure 3-10: bidirectional boost DC-DC converter circuit diagram

The parameters of the component of the converter have been chosen based on the following MATLAB code:

```
%% inputs
P= 1000000;   % 1MW
Fs= 100000;   % 100 KHz
Vo= 1500;
Vin_min= 500;
Vin_max= 1500;
Vin_avg = 1000 ;
D= (Vo-Vin_avg)/Vo;
I= P/1500;
R= P/I^2;
L= (D*Vin_avg*Vin_avg)/P/0.4/Fs;
C= D*Vo/0.01/R/Fs;
```

The two switches are controlled by pulse width modulation with a duty cycle D, switch one S1, is the output signal of the PWM while switch two S2 gives the complement signal. Hence, when S1 is on, S2 is off and vice versa.

3.2.4 Controlled Closed loop circuit

To control the DC voltage and maintain it at the desired level without being affected by the input voltage fluctuation, the converter is connected in closed loop circuit where a feedback from the output voltage is compared to a reference value of voltage

and the error- difference- is sent to PI regulator to adjust the value of the duty cycle accordingly until we get the desired level of voltage.

The PI regulator was tuned automatically by Simulink starting from initial values kp=ki=1, and PI parameters kp and ki were set to 0.005 and 2 respectively. Fig. 3-11 shows the circuit of the closed loop

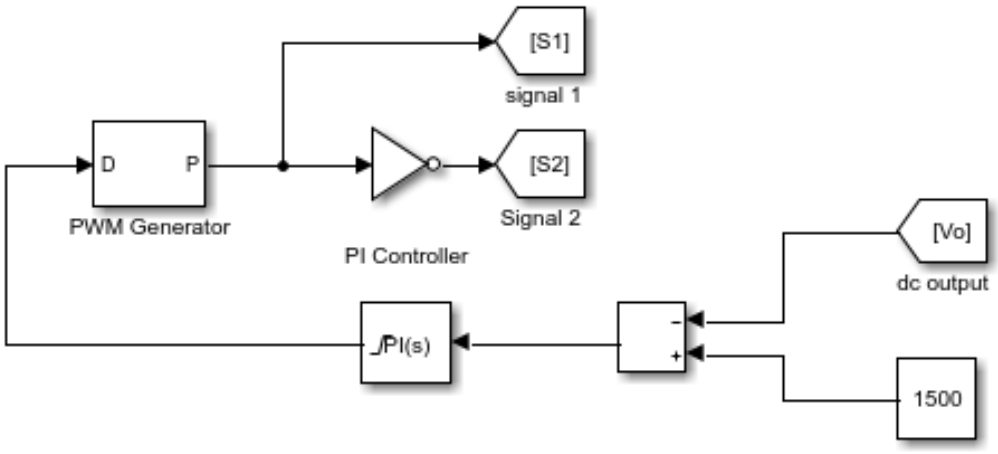

Figure 3-11: closed loop control with PI regulator

Another PI tuning method can be analyzed starting from the open loop system transfer function:

$$G(S) = (k_p + \frac{k_i}{s}) * \left(\frac{R}{s^2CLR+sL+R}\right) = \frac{R*(k_p+\frac{k_i}{s})}{s^2CLR+sL+R} \qquad (3.6)$$

The close loop transfer function will be:

$$W(s) = \frac{G(s)}{1+G(s)} = \frac{\frac{R*(k_p+\frac{k_i}{s})}{s^2CLR+sL+R}}{1+\frac{R*(k_p+\frac{k_i}{s})}{s^2CLR+sL+R}} = \frac{k_p(s+\frac{k_i}{k_p})}{sCL*\left(s^2+\frac{sL}{CLR}+\frac{R}{CLR}\right)+k_p(s+\frac{k_i}{k_p})} \qquad (3.7)$$

Since the system gain at cutoff frequency is 3Db ≈ 0.7:

$$\|W(\omega_{cut})\|^2 = \left[\frac{R*(jk_p\omega+ki)}{(-j\omega^3CLR-\omega^2CL^2+j\omega(CLR+k_p)+k_i)}\right]^2 \approx 0.5 \qquad (3.8)$$

Solving the previous equation using MATLAB for we can get ki and kp.

By setting the reference voltage to a desired voltage level of 1500 V, and running the simulation the following voltage waveform fig. 3-12 is resulted. It exhibits the voltage is regulated after a short transient. It can be seen that there is a small voltage ripple less than 0.1 V at the output DC voltage which might be reduced by increasing the capacitance.

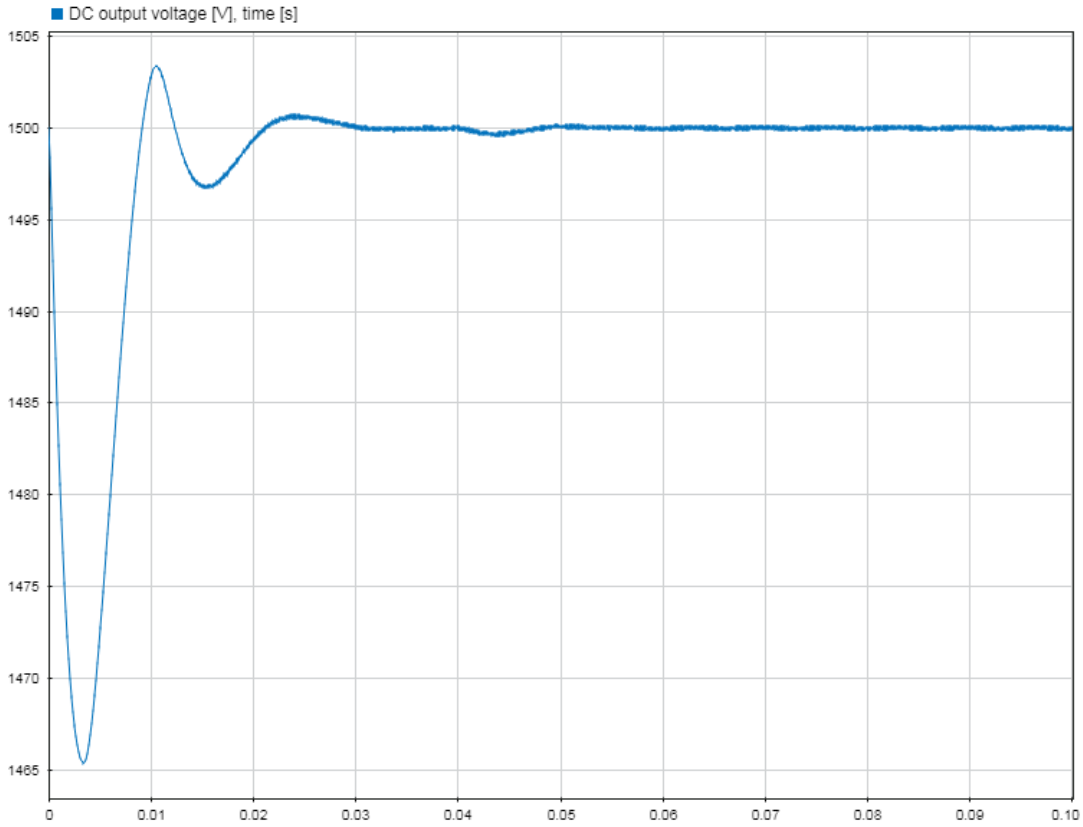

Figure 3-12: converter output DC voltage before implementing the closed loop circuit

3.3 DC AC Inverter

A three phase two level voltage source inverter VSI has been selected and modelled as shown in fig. 3-13. The input side of the inverter is connected to the regulated DC voltage coming from the DC-DC converter. Each leg of the three phase bridge inverter is controlled through sinusoidal pulse width modulation (SPWM) with phase delay of 120 degrees. This will result in output voltage which is square wave pulses with two levels of voltages Vdc/2 and – Vdc./2

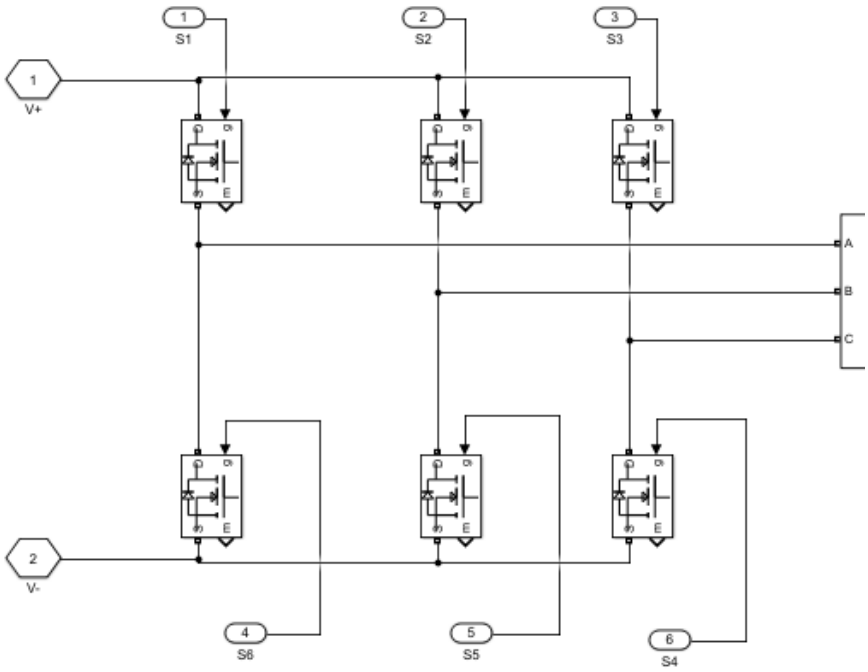

Figure 3-13: three phase –two level VSI circuit diagram

3.3.1 SPWM:

As mentioned above, the control of the inverter is done by SPWM controller; the SPWM technique has been chosen as one of the most popular techniques. It compares a sinusoidal reference signal (at desired frequency so called, the fundamental frequency) with a triangular carrier signal (at a switching frequency) as shown in fig 3-14 and 3-15. The modulation frequency Mf is chosen as the ratio of switching frequency to fundamental frequency, and it has to be an integer so that to avoid inter-harmonics. And need to be a multiple of three to get rid of harmonics that are in the order of multiple of three [1].

The modulation frequency has been chosen as Mf= 201 so that the switching frequency of the triangle signal was is 201 times the fundamental frequency 50 Hz, the three sinusoidal reference signals S have an amplitude of 1, and frequency 50 Hz which is the desired frequency for the inverter output voltage and 120 degrees phase shift from each other. When the control signal S1 is greater than the triangle signal St the switch is on and when S1 is less than St Switch is off. This will result in switching output voltage as shown in fig 3-16

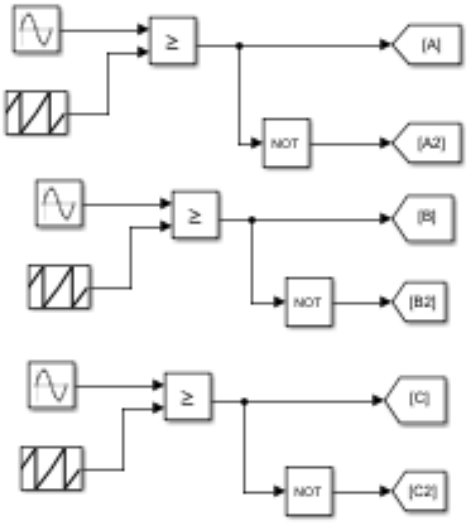

Figure 3-14: SPWM technique

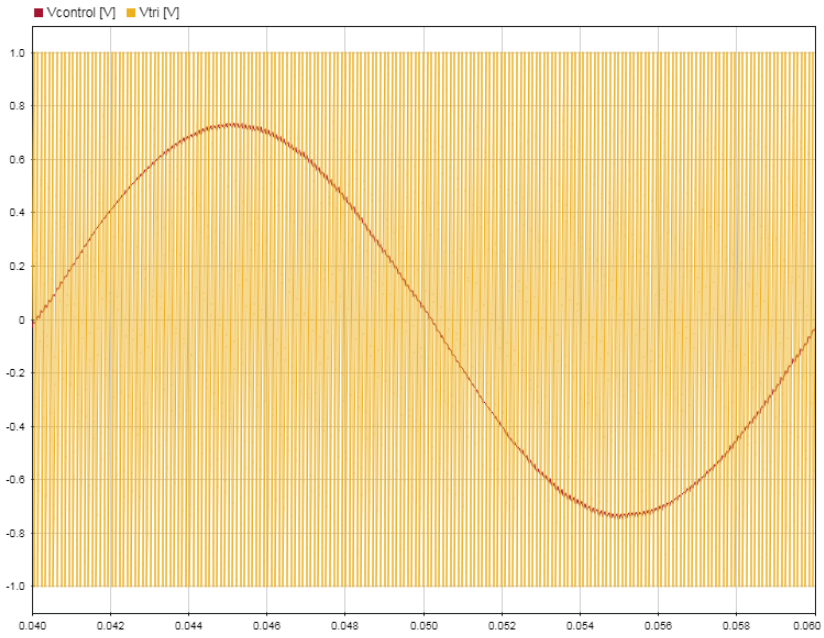

Figure 3-15: generation of SPWM switching signal by comparing the fundamental signal with the carrier signal

The resulted switching signals A, B and C for the upper switch in each leg are shown in fig. 3-16, while for the lower switches the complement were taken.

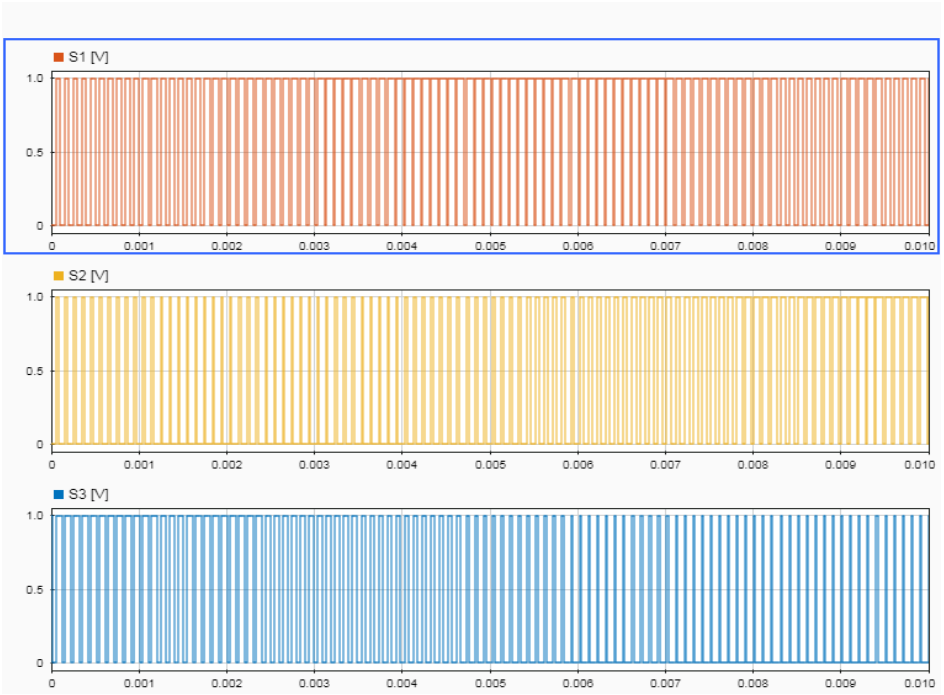

Figure 3-16: switching signal of the inverter for each phase

The output voltage of the inverter accordingly will be switched pulses with amplitudes of Vdc/2 and – Vdc/2, and width of the pulses following the modulation signal. The voltage and current waveform are depicted in fig. 3-17

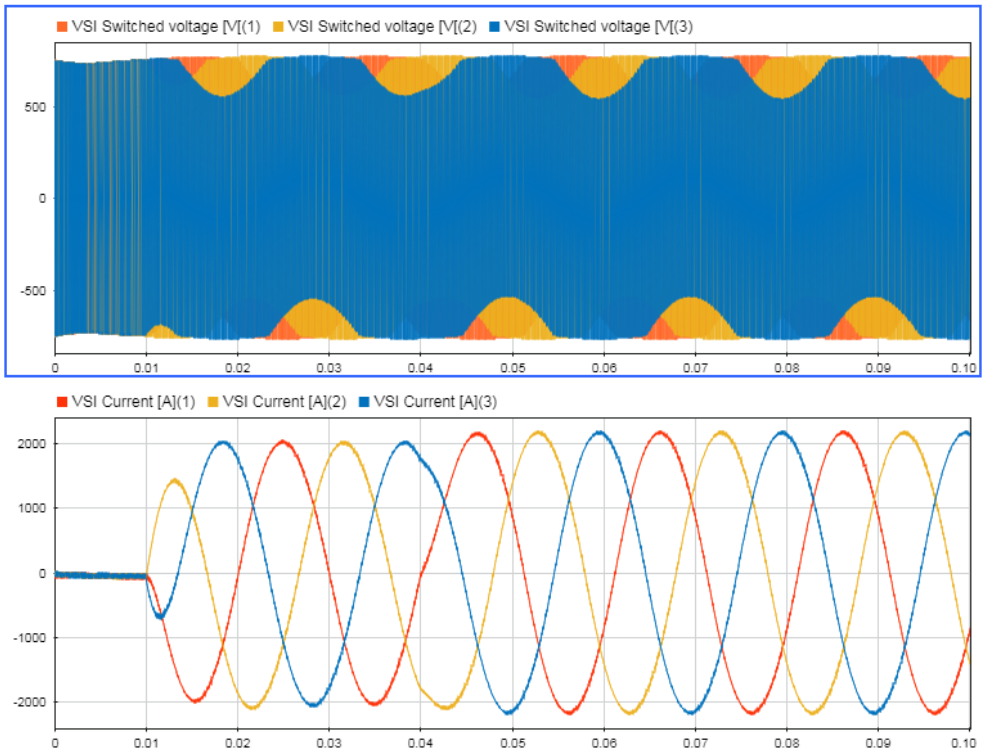

Figure 3-17: inverter output switched voltage waveform and current

3.3.2 L filter design

The switching harmonics resulted from the VSI require the connection of a filter. Hence, L filter has been chosen as the simplest and preferred filters when it comes to VSI operations, but L filters become bulky and costly when used for low switching frequencies [6].

The value of the inductor of the filter is chosen based on the switching frequency and the maximum acceptable current ripple. In the model the inductor value was set to 0.5 μH. The schematic diagram of the filter connected to the VSI is shown in Fig. 3-18.

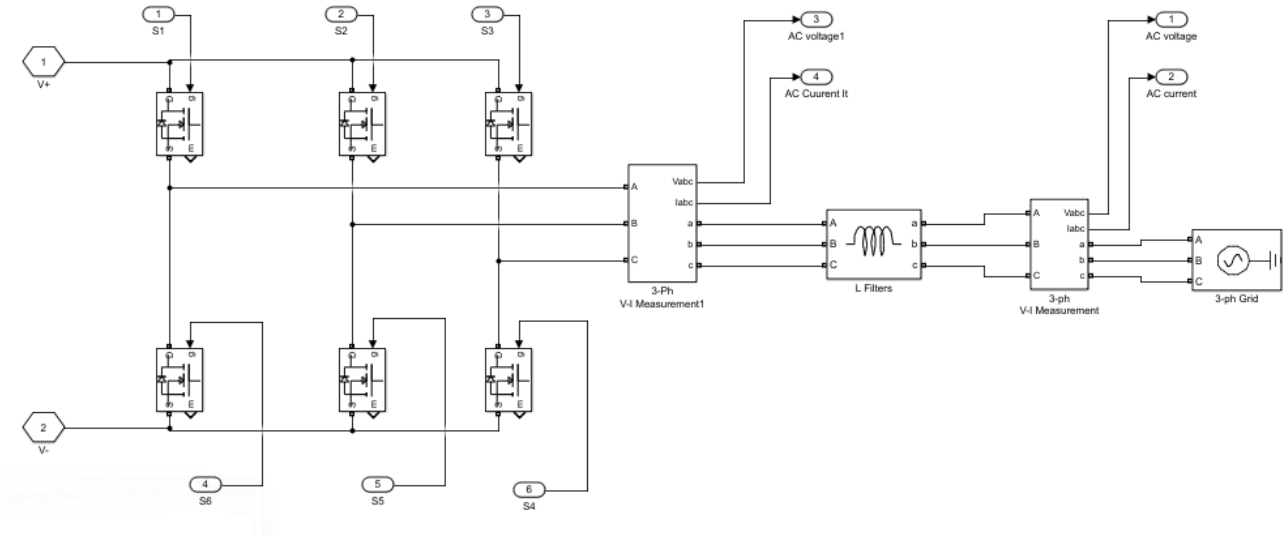

Figure 3-18: Filter schematics diagram connected at the inverter output

The acquired voltage and current waveforms resulted after connecting the filter are shown in fig. 3-19 below, from the waveform it can be seen that the filter attenuates the harmonics and gives a pure three phase sinusoidal voltage with 50 Hz and around 327 V peak, has been achieved.

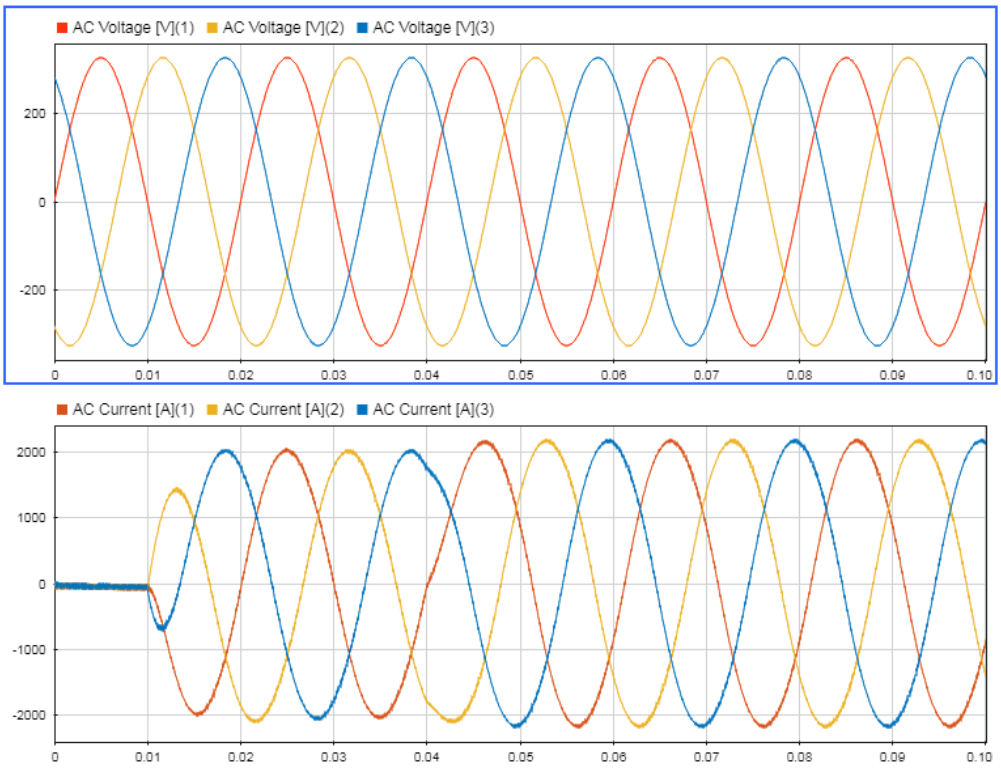

Figure 3-19: sinusoidal voltage and current waveform after connecting the filter at the inverter side

It can be seen that the voltage and current waveform are out of phase and hence a phase locked loop PLL control is modeled as illustrated in fig. 3-20. The inverter output AC voltage is transformed from ABC reference frame to DQ0 reference frame to simplify and facilitate the control system. The Q component of the voltage is compared with zero reference and sent to PI controller which has been tuned automatically using Simulink, and that adjusts the angular frequency accordingly. The angular frequency is then integrated to get the phase.

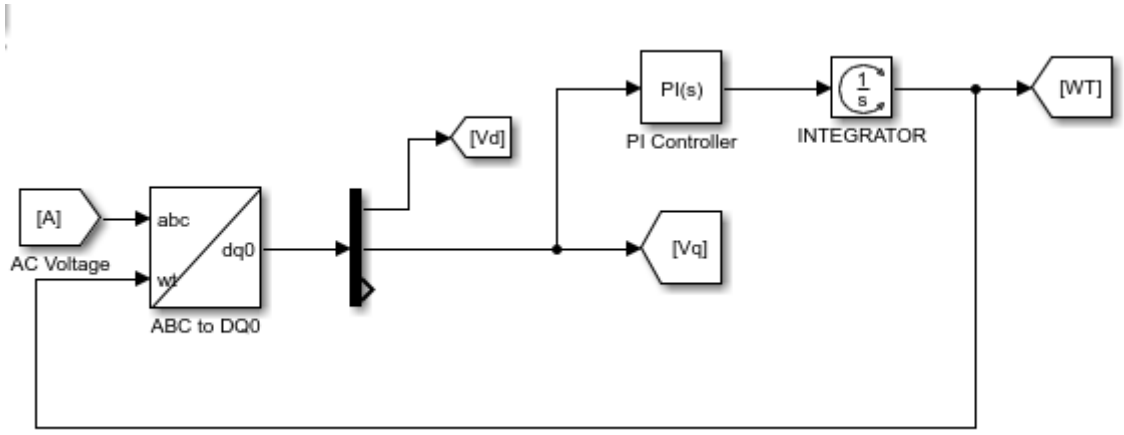

Figure 3-20: Phase locked loop

The AC voltage DQ components resulted from the PLL with zero Q component reference are depicted in fig. 3-21

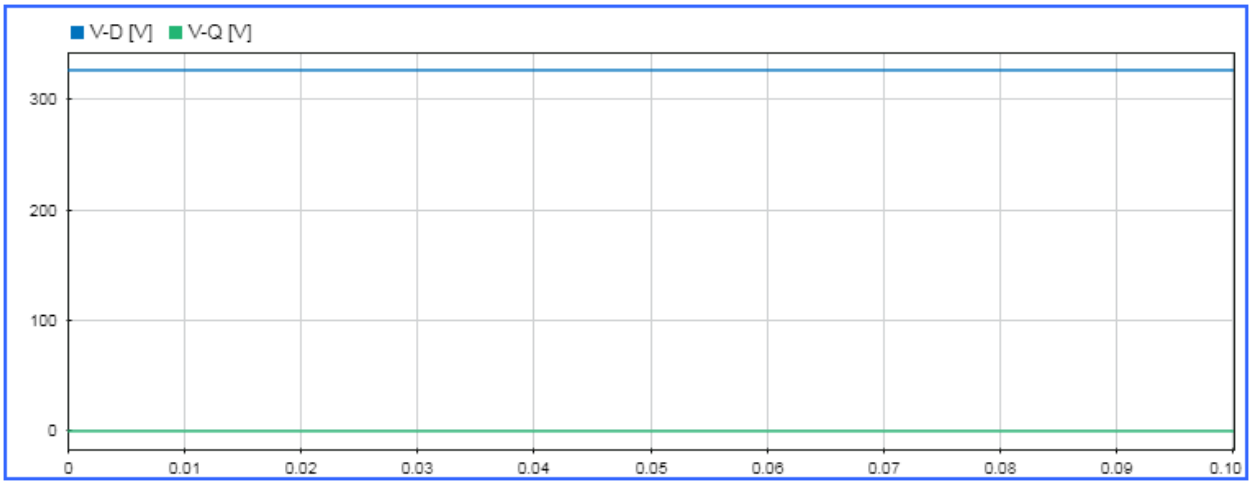

Figure 3-21: D-Q component for the AC voltage at the grid side

3.3.3 Active and reactive power Closed loop control

A current control scheme has been chosen because it's more robust and necessary to avoid overcurrent - to control the power at the grid side. The control

scheme was implemented in D-Q reference frame. The three phase output voltage and current at the grid side were measured and then transformed from ABC reference frame to D-Q reference frame. The Vd and Vq quantities are entered to PLL control to control the real and reactive power. For zero reactive power, the current need to be in phase with voltage so cosθ =1. To achieve this condition, Vq is put equal to zero.

The measured output current was also transformed from ABC reference frame to D-Q reference frame using the phase resulted from the PLL controller. For the closed loop current control, a reference D – Q current component were calculated from the real and reactive power. Then these current references were compared with the actual D –Q current components from the inverter output current. The error is sent to PI controller that acts as a compensation to track the DC current references thus the open loop transfer function can be represented by the following equations:

$OL(s) = K(s) * \frac{1}{L*s+(R+r_{on})}$ Where K(s) is the PI gain → k(s) = kp+ki/s

$$OL(s) = \frac{k_p/L}{s} \frac{s+{k_i}/{k_p}}{s+(R+r_{on})/L} \quad (3.9)$$

By imposing that the closed loop transfer function equals $CL(s) = \frac{1}{\tau*s+1}$ the PI parameters result as follows:

$$k_p = \frac{L}{\tau} \quad (3.10)$$

$$k_i = \frac{R+r_{on}}{\tau} \quad (3.11)$$

Where:

τ : time constant of the closed loop system

L: inductance of the filter

R: resistance at the grid side

ron: on resistance of MOSFETs

The values then for k_p and k_i were found to be 0.25 and 50 respectively.

The voltage resulted from the PI controller was then added to the grid voltage components and the DQ current components multiplied by (L*ω=0.5*10^-3*2pi50) as

feed forward action. The resulted voltage is the voltage at the inverter side which is then divided by Vdc/2 to get the modulation signal D –Q components. The model of the current control scheme is illustrated in fig. 3-22. The modulation signal MD and MQ are then transformed back to ABC reference frame and sent to the SPWM to generate the switching signals accordingly, this is shown if fig. 3-23 and the generated modulation signal are three phase voltage adjusted by the closed loop control accordingly as shown in fig. 3-24.

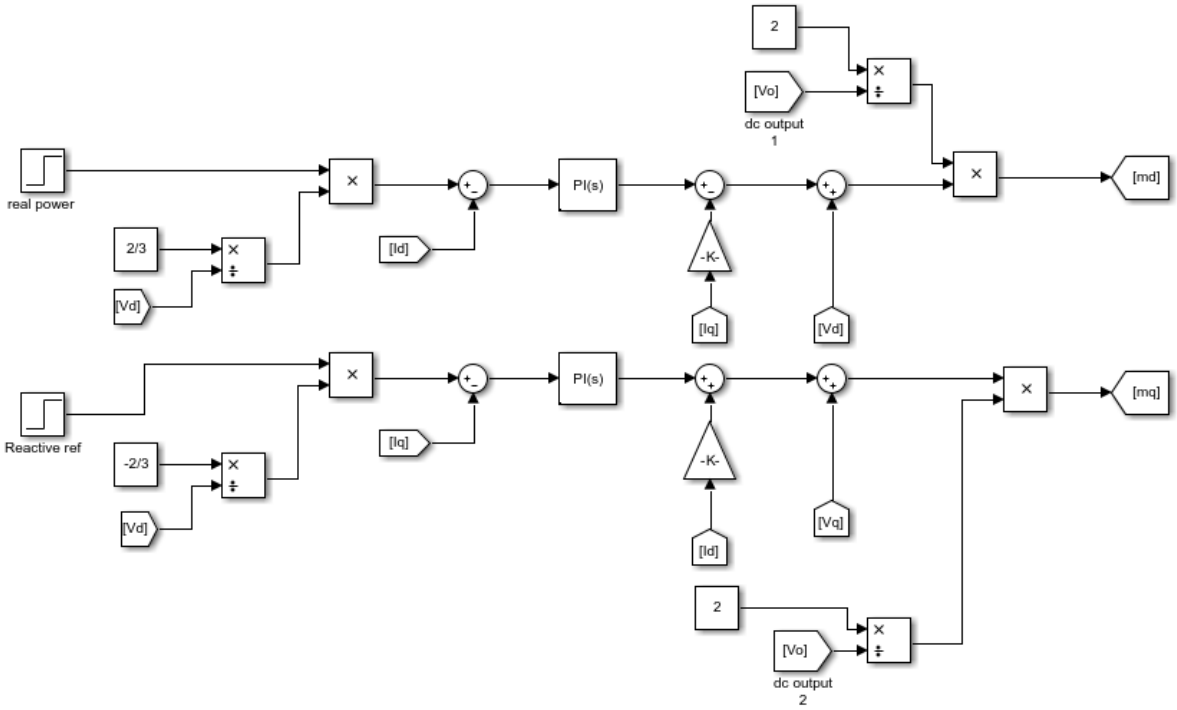

Figure 3-22: Closed loop current control scheme for controlling real and reactive power

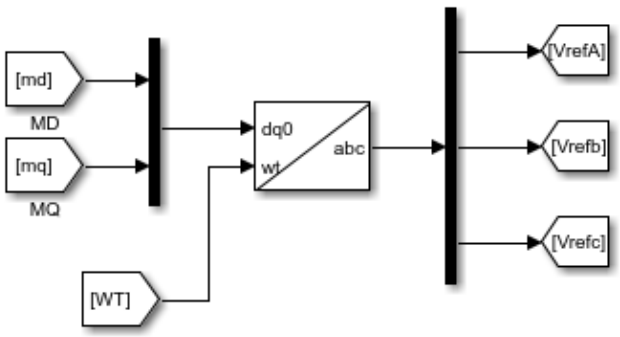

Figure 3-23: Modulation signal reference

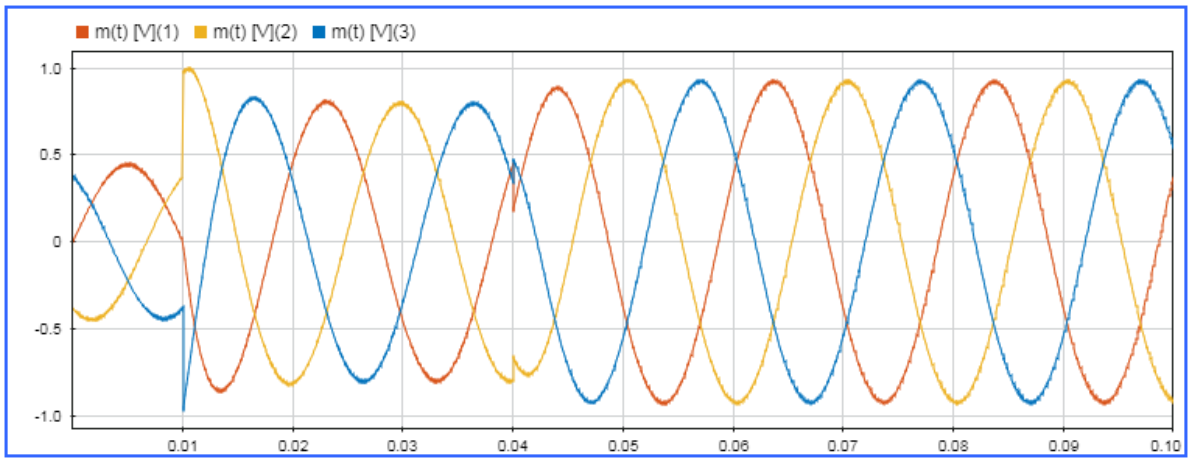

Figure 3-24: Modulating signal

The resulted D-Q components for the AC current after implementing the current control scheme must be equal to the reference values based on the real and reactive power references. Considering 1 MW real power and zero reactive power for the time 10 to 40 ms and then injecting 0.4 MVAR reactive power in the grid, the current D-Q components can be shown in fig. 3-25 below, while real and reactive power are shown in fig. 3-26.

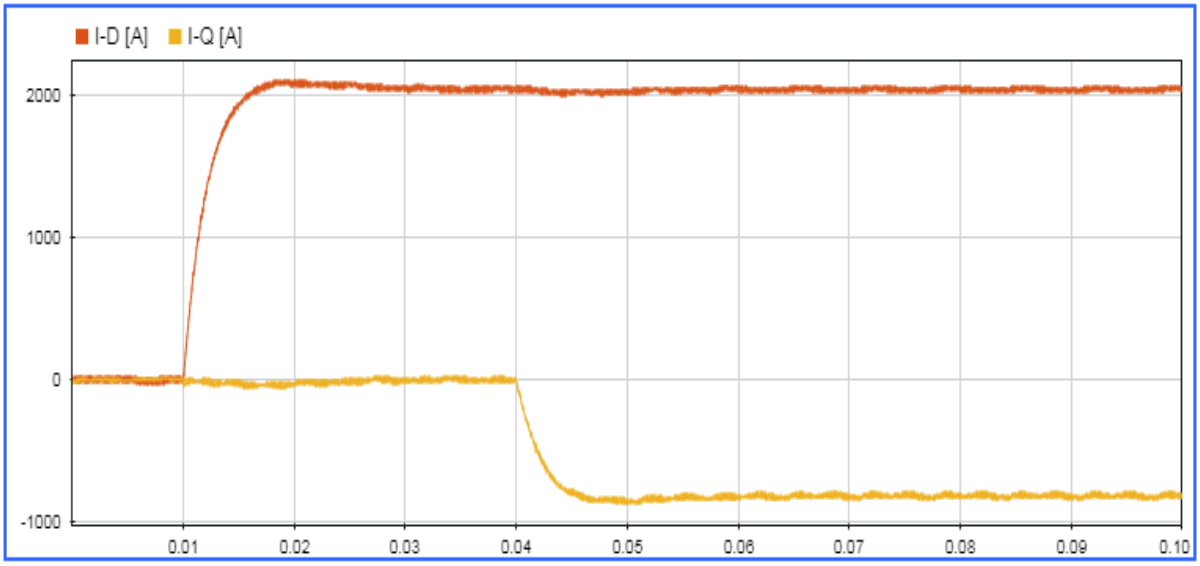

Figure 3-25: D-Q current component resulting from the current control scheme

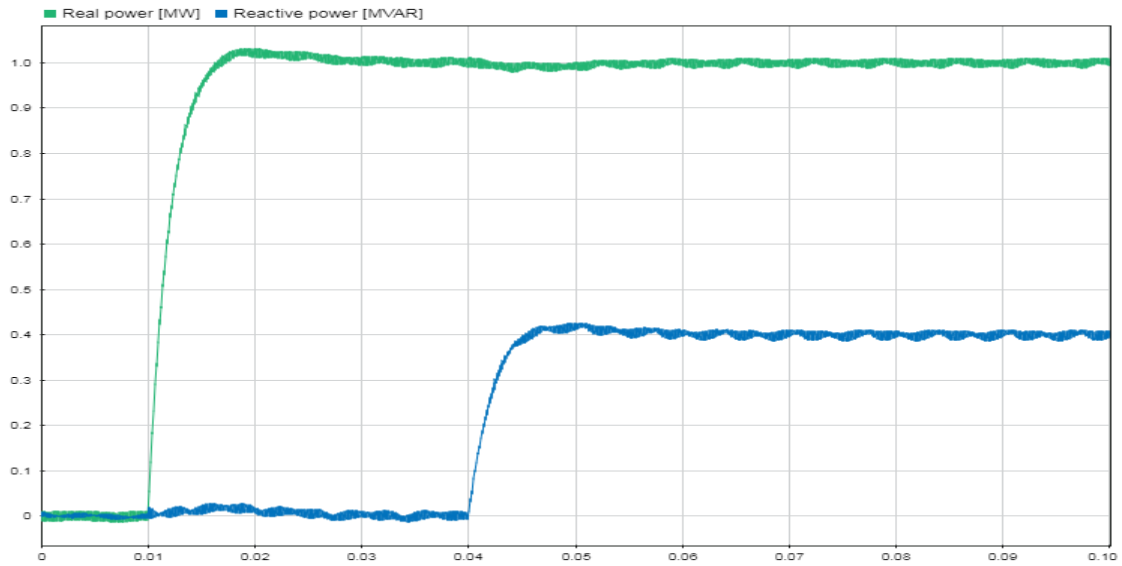

Figure 3-26: per unit real power and reactive power resulting from the current control scheme

Conclusion

The present study focused on analysing the use of DC-DC convertor and DC-AC inverter connected to three phase grid system. The study modelled the overall system from the energy storage device up to the three-phase load.

The modelling of power electronics converters interfaced to three phase grid has been implemented as follows: Starting from Energy Storage System represented by supercapacitor model, an output DC voltage is acquired. The regulation of the DC voltage has been done through the DC-DC converter, different scenarios for DC-DC converters have been experimented and boost converter was found to be the simplest and optimum solution to implement. Accordingly a bidirectional boost converter has been modelled to allow the energy flow from both sides and designed with the most suitable choices for the passive components. A closed loop control system was connected to the converter in order to maintain and control the output DC voltage at the desired level in case of input voltage fluctuations.

The next step was to model the DC-AC side and a VSI has been modelled and controlled with SPWM considering under modulation. Then, in order to get a sinusoidal AC voltage at the output, L filter has been connected at the output of the inverter side to eliminate the harmonics and generate a sinusoidal signal to be seen by the grid side. A closed loop current control scheme was connected to the inverter to control the real and reactive power and maintain the output AC voltage for the load at the desired frequency and amplitude.

The analysis concluded that:

- Different scenarios to regulate the DC voltage and control the output, choosing of the passive component, how to go to bidirectional model and implementation of non-switching model.
- Implementation of SPWM to get 50 Hz, 400 V rms AC voltages and interface it to three-phase grid system.
- Closed loop current control applicable for real and reactive power control.

- The simulation and results demonstrated the ideal behaviour of the system with a simple and feasible model.

The scope of this thesis work might be broadened and continued to incorporate a grid model from the load side, as well as simulation and modeling of the ESS and means of generation, such as photovoltaic (PV) panels or hybrid generation.

Bibliography

[1] 1995_BOOK_Mohan_820p_Power_Electronics_2nd

[2] Robert W. Erickson, Dragan Maksimović - Fundamentals of Power Electronics - Springer US (2004)

[3] Yazdani and Iravani - Voltage-sourced converters in power systems_ modeling, control, and applications (2010)

[4] M. Krpan, I. Kuzle, A. Radovanovic and J. V. Milanovic, "Modelling of Supercapacitor Banks for Power System Dynamics Studies," in IEEE Transactions on Power Systems, doi: 10.1109/TPWRS.2021.3059954.

[5] M. A. Elsaharty and H. A. Ashour, "Passive L and LCL filter design method for grid-connected inverters," 2014 IEEE Innovative Smart Grid Technologies - Asia (ISGT ASIA), 2014, pp. 13-18, doi: 10.1109/ISGT-Asia.2014.6873756.

[6] U. P. Yagnik and M. D. Solanki, "Comparison of L, LC & LCL filter for grid connected converter," 2017 International Conference on Trends in Electronics and Informatics (ICEI), 2017, pp. 455-458, doi: 10.1109/ICOEI.2011